AN ABSTRACT OF THE THESIS OF

Cha, Jae Kyung for the degree of Master of Science in Forest Products presented on March 21, 1985.

Title: Effect of Loading Rate on Damping and Stiffness in Nailed Joints

Redacted for Privacy

Abstract approved: _____
Anton Polensek

The conventional studies for nailed joints vary and no standard methods exist for evaluation of damping in wood joints. Wood buildings experience earthquake-caused oscillation of three or more Hz, but damping values used in design are based on static test. To evaluate damping at loading rates associated with earthquakes, cyclic-load tests were conducted on single-nail joints of wood and plywood. The investigated loading rates were between the static ASTM rate and sine function of 15 Hz.

The results showed that damping ratio increased with the frequency-associated loading rate between the static ASTM rate and 4 Hz, then it gradually decreased as the rate was increased to 15 Hz. Another variable, load level, influenced damping ratio at all rates except for 1 Hz. Observation was also made on nail stiffness: at high load level, slip moduli consistently increased

between the static ASTM rate and 15 Hz. At low load level, it increased between the ASTM rate and 2.5 Hz and decreased between 2.5 and 15 Hz. Statistical analysis showed that both, damping ratio and slip modulus weakly correlated with loading rate, while work capacity, dissipated energy and total slip displayed strong correlation.

Effect of Loading Rate on Damping and Stiffness in Nailed Joints

by

Cha, Jae Kyung

A THESIS

submitted to

Oregon State University

in partial fulfillment of
the requirements for the
degree of

Master of Science

Completed March 21, 1985

Commencement June 1985

APPROVED:

Redacted for Privacy

Professor of Forest Products

in charge of major

Redacted for Privacy

Head of Department of Forest Products

Redacted for Privacy

Dean of Graduate School

Date thesis is presented March 21, 1985

ACKNOWLEDGEMENTS

It is my pleasure to express my appreciation to my major professor, Dr. Anton Polensek, for his encouragement, patience and advice. Without his assistance this project would have never been completed.

I would like to express special appreciation to Dr. H.R. Holbo for his assistance with testing instrumentation.

I also wish to thank Boyd Schimel for his helping in computer work and Ken Bastendorff for his assistance in testing arrangement.

I would like to thank Dr. R. Petersen, Dr. M. Corden and Dr. P. Humphrey for serving on my committee; and Dr. H. Resch and Dr. M. McKimmy for reading the thesis and providing many helpful suggestions.

Finally, I would like to express thanks to my wife, Jean-ok, for encouraging my work to carry out my studies.

TABLE OF CONTENTS

I. INTRODUCTION 1

II. LITERATURE REVIEW 4

2.1 Parameters Affecting Nail Behavior 4

2.1.1. Types of Joints 5
2.1.2. Joint Strength and Stiffness 7
2.1.3. Damping in Nailed Joints . . 8
2.1.4. Methods of Measuring Structural Damping 10

2.1.4.1. Damping by Free-Vibration . . 11
2.1.4.2. Damping by Static Cyclic Test . . . 14

2.2 Discussion of Pertinent Literature 19

III. MATERIALS AND METHODS 23

3.1 Experimental Design 23

3.2 Material Selection and Conditioning 25

3.2.1 Studs 25
3.2.2 Sheathing Material 26
3.2.3 Nails 26

3.3 Specimen Construction 28

3.4 Testing Arrangement 31

3.4.1 Specimen Mounting 31
3.4.2 Loading Functions 32
3.4.3 Arrangement for Applying Load Functions 33
3.4.4 Data Acquisition Arrangement 33
3.4.5 Testing 35

Table of Contents--continued

IV. RESULTS AND DISCUSSION 40

4.1 Reduction of Experimental Data . . . 40

4.1.1 Data Description 40
4.1.2 Procedure for Data Reduction 44
4.1.3 Statistical Analysis 48

4.2 Relation Between Damping Ratio and Loading Rate 48

4.3 Relation Between Stiffness and Loading Rate 57

V. CONCLUSIONS AND RECOMMENDATIONS 67

BIBLIOGRAPHY 69

APPENDICES 72

Appendix A Computer Program for Data Reduction 73

Appendix B Scattergram of Damping Ratio 79

Appendix C Results from T-Test . . 84

LIST OF FIGURES

Figure		Page
2.1.	Load Transfer and Slip Damping in Wood Joints	9
2.2.	Vibration Model for Single Degree-of-Freedom System	12
2.3.	Amplitude-Time Relationship from Free Vibration Test	12
2.4.	Load-slip Curve for Fully Reversed Force	16
3.1.	Specimen Construction and Testing Arrangement	29
3.2.	Block Diagram for Arrangement of Load Control and Data Acquisition	34
3.3.	Block Diagram Used in Data Acquisition	36
3.4.	Diagram for Ramp Loading	38
3.5.	Diagram for Sinusiodal Loading	39
4.1.	A Typical Load-Slip Trace, Obtained by an X-Y Recorder, of Sample No. 3 with 1-Hertz Sine Loading	41
4.2.	A Typical Load-Slip Trace, Obtained by a Data Acquisition System, of Sample No. 3 with 1-Hertz Sine Loading	42
4.3.	A Typical Load-Slip Trace, Obtained by a Data Acquisition System, of Sample No. 7 with 10-Hertz Sine Loading	43
4.4.	A Typical Digitized Load-Slip Trace	46
4.5.	Relationship between Damping Ratio and Loading Rates	56

LIST OF TABLES

Table		Page
3.1.	Description of Samples and Loading Types	24
3.2.	Classes of Probability Density for Modulus of Elasticity and Specific Gravity of Lumber	27
4.1.	Number of Useful Traces	45
4.2.	Dissipated Energy, Work Capacity and Damping Ratio	49
4.3.	Analysis of Variance for Effects of Load Levels and Loading Rates on Damping Variables	50
4.4.	Analysis of Variance for Effect of Load Levels on Damping Variables	52
4.5.	Analysis of Variance for Effect of Loading Rates on Damping Variables	53
4.6.	T-Test for Damping Ratios and Loading Rates	55
4.7.	Regression Equations Relating Joint Properties and the Effect of Load Level and Loading Rate	58
4.8.	Statistics of Slip Moduli for Samples Investigated	59
4.9.	Analysis of Variance for Effect of Load Levels and Loading Rates on Joint Slip and Stiffness	61
4.10.	Analysis of Variance for Effects of Loading Rates on Slip Modulus and Total Slip	62
4.11.	Analysis of Variance for Effect of Load Level on Slip Moduli and Total Slip	63
4.12.	Statistics for Total Slip Expressed in Inches	64
4.13.	Regression Equations Relating Joint-Slip Properties to Load Level and Loading Rate	66

EFFECT OF LOADING RATE ON DAMPING AND STIFFNESS IN NAILED JOINTS

I. INTRODUCTION

Damping and stiffness of nailed joints greatly affect the overall structural reliability of light-frame wood buildings. Damping is the result of energy dissipation during vibration caused by dynamic loads due to earthquakes and winds. Therefore, damping is an essential property in the theoretical analysis of structural performance. Such an analysis is complicated, because wood structures behave inelastically, which is characterized by reduced modulus of elasticity as the loads get larger.

Under cyclic loading, structural systems that dissipate energy display the load-deformation traces as hysteresis loops. The energy dissipation is easily evaluated from these loops, which is in turn used to determine damping. In milti-degree-of-freedoms, such as light-frame wood buildings, evaluation of damping utilizes the concept of equivalent viscous damping. The traditional concept of viscous damping is valid for single-degree-of-freedom linear systems [17, 18]. However, wood systems are inelastic and have many degrees of freedom. Therefore, Jacobsen [12, 13] extended the concept for the single-degree elastic system to the multi-degree system by assuming that damping and mass

properties are lumped into a single-degree system that has the same properties as the original multi-degree system. For instance, the coefficient of viscous damping in the equivalent single-degree system is based on the total energy dissipated in the multi-degree system. This concept, based on the equivalence of dissipated energy in both systems, defines the damping ratio that is proportional to the velocity of the vibrating system. At low loads, when the wood system behaves elastically, the equivalent viscous damping ratio provides realistic measure of energy dissipation [17, 18].

The main source of damping in build-up structures is interlayer friction in joints. Wood buildings belong to such structures. They are composed of components that are in close contact at joints which dissipated energy as the building deflects under loads. This energy dissipation or damping is especially important when the loads are dynamic, such as those caused by earthquakes and winds. The coefficient of damping in systems with nailed wood joints is about 10% [4, 17, 18], while that of wood material is only about 0.35% [30, 31]. The known damping properties are mostly associated with specific wood systems and not with joints where the damping takes place. Consequently, information is needed on damping in the most common wood joints, such as

nailed joints of light-frame wood buildings.

One reason for a limited information on damping is a large variety of nailed joints. Most of the existing studies on joints are limited to the strength properties with nails driven perpendicular to the grain [22]. Another reason is nonlinear behavior which complicates the testing and data evaluation for damping and stiffness [22]. There is a need to define the nonlinear properties in such a way to be easily used in the theoretical analysis of components in wood buildings [22].

Several investigations [22, 24] show that the loading rate during testing affects damping. The damping ratio in nailed joints tested at 1.0-hertz rate was observed to be about 31% and at 0.1-hertz rate was about 22%. The effect of loading rate at frequencies above 1.0 hertz has not been studied. Because wood buildings experience earthquake-caused oscillations higher than 1.0 hertz, additional investigations are needed on correlation between the loading rate and damping ratio.

The main objective of this study was to develop the relation between the loading rate and damping ratio. Another objective was to evaluate the effect of loading rate on slip modulus.

II. LITERATURE REVIEW

A large number of studies have been conducted on nailed joints. The studies are varied by the objectives and testing arrangements. Furthermore, in light frame wood buildings, there are numerous types of joints which are characterized by many species of lumber, sheathing types and nail types. Therefore, it is difficult to evaluate literature from a common perspective.

This chapter deals with the parameters affecting nail behavior and contains a discussion of pertinent recent research findings.

2.1. Parameters Affecting Nail Behavior

Wood is a natural material, so variation in wood properties occurs not only among species but also within a given species and within a single board. Other characteristics that influence wood properties are moisture content, direction of grain and specific gravity. Wood properties in turn influence joint properties. The main characteristics affecting nailed joints are specific gravity and moisture content. Specific gravity influences the elastic bearing constant of wood which is directly related to the stiffness of nailed joints [27].

2.1.1. Types of Joints

The strength and stability of any structure depend heavily on the fastenings that connect the components together. A wide variety of mechanical fasteners exist for light-frame wood structures: nails, screws, spikes, metal plates and staples. Each fastener produces joints with different strength and stiffness properties. Additional effects on joint properties come from wood properties and joint geometry.

Nails are the most common mechanical fasteners used in wood construction. They resist either withdrawal or lateral loads, or a combination of both. Properties of nail joints are influenced by nail characteristics, such as diameter, length, size and shank type. Joint properties are also influenced by characteristics of connected materials, such as species, dimensions of connected member, grain orientation, defects and by characteristics of joint configuration, such as nail spacing, number of nails and interlayer gap between members.

Spikes are mechanical fasteners similar to nails by the manner in which they are manufactured and used. They are heavier and designed to transfer larger loads than those of nails. They have either a chisel point or diamond point.

The second most important mechanical fasteners perhaps are staples which are available in clips and magazines to permit application by pneumatically operated portable staplers. Most characteristics that affects the withdrawal and lateral loads of staples are similar to those of nails.

In resisting withdrawal forces, wood screws are superior to nails and staples. The common types of wood screw have flat, oval or round heads. The flathead screw is most commonly used, if a flush surface is desired. Ovalhead and roundhead screws are used for appearance, and roundhead screws are used when countersinking is objectionable. Lag screws are used for structural applications when large forces are transmitted. Lag screws may be used instead of bolts when it is difficult to fasten bolts or where nuts on the surface are objectionable.

Several types of connectors have been devised that increase joint bearing and shear area, among which rings and plates, combined with bolts, are the most important. The primary load carrying portions of joints are rings or plates, while the bolts serve to prevent sideway separation of members and their contribution to load carrying capacity is marginal.

2.1.2. Joint Strength and Stiffness

One of the desirable features of wood as a construction materials is the simplicity of making its joints. Among the mechanical devices used in wood to wood connections, none is so widely popular as nails.

Although nailed joints appear to be simple in appearance, their properties are quite complex. Usually, the properties are obtained by applying load to representative joint specimens and measuring the resulting deformation or slip. A comprehensive review of the load-slip behavior of nail joints was presented by Antonides et al. [3].

Recently, emphasis has been placed on the evaluation of load-slip traces obtained from testing of one-nail joints under lateral loading [22]. Such load-slip traces of joints between lumber and most sheathing materials are non-linear except for a very small initial part of the trace. This linear part is often used to define the joint stiffness in terms of slip modulus defined by the initial tangent on the load-slip trace. The nonlinear parts are characterized by the decreasing slope of the trace under increasing load; they may be represented either by linear slip moduli that are valid between two slip levels or by nonlinear functions fitted to experimental traces.

2.1.3. Damping in Nailed Joints

Damping in nailed joints is governed by the degree of interface friction. In order to predict the damping of a given structure, all possible damping sources do not have to be included, because one or two sources usually predominate, while the effect of others is negligible.

Yeh described the shear transfer between two word elements as follows [30, 31]. Nail-connected structural elements are subjected to interface pressure, N (Fig. 2.1). Under shear load, F, relative interface motion occurs, which depends on N and F and on the loading history. This loading subjects the nail to the combined shear and flexual forces which are distributed nonlinearly along the nail length. When load F is increased at small increments, ΔF_i, and F becomes large enough, small regions of interface undergo plastic deformation. The total tangential force is:

$$F = \sum_{i=1}^{n} \Delta F_i \quad . \quad . \quad . \quad . \quad . \quad . \quad . \quad . \quad . \quad . \quad . \quad (2.1)$$

ΔF_1 produces a slip, ΔL_1 (y), over a region along the loaded edge of the interface. Incremental slips result in overall slip, $L_T(y)$, as ΔF_1, ΔF_2, ΔF_3 . . . ΔF_n are added together and F is transmitted through the interface. The mechanisms of transfer of each ΔF, depends

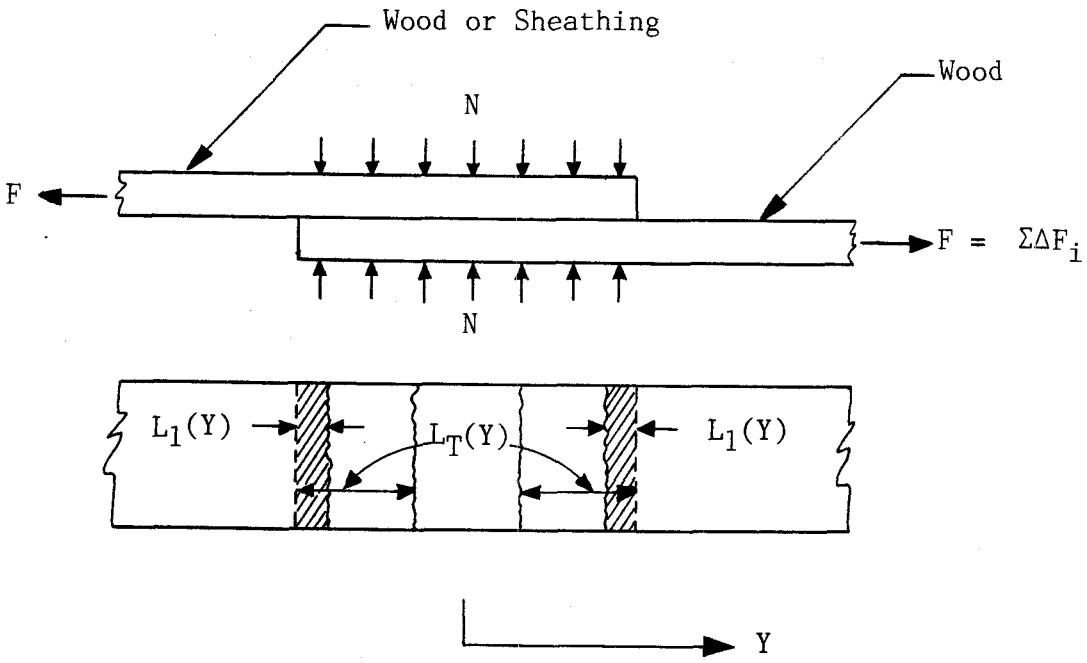

Figure 2.1. Load Transfer and Slip Damping in Wood Joints

on the N, the coefficient of friction, and in nonlinear case on the current value of the accumulated F.

The interlayer slip first occurs at the edges of wood and sheathing, which are perpendicular to F and then it propagates inward. This slip deforms and tilts the nail which becomes inelastic when F gets large enough.

During unloading from F to zero, reverse slip occurs, again beginning at the same two edges. The unloading may be visualized by incremental reduction of shear force until all the load is removed.

Under cyclic loading of constant amplitude, the plastic deformed regions around nails of connected material grow with each cycle; an appreciable amount of plastic deformation develops in the wood and nail, and hence the energies are dissipated in the wood and the nail. The energy dissipated depends on F, interlayer thickness and breadth, coefficient friction, specific gravity of wood and sheathing, and the degree of plastic deformation. Clearly such an effect is not linear damping.

2.1.4. Methods of Measuring Structural Damping

Two major methods are commonly employed to evaluate damping ratio, free-vibration and static cyclic method. Other methods, such as equilibrium method,

energy input method, and lateral deflection method [14, 17] are used when damping is small. They are not used in this study, because damping in wood joints is large.

2.1.4.1. Damping by Free-vibration. The treatment of this subject, available in many textbooks on vibration, is summarized next. Dynamic loads cause deflections which vary with time and produce vibration which can be classified according to the forces that cause motion. Free-vibration, caused by initial displacement, velocity or acceleration, has no external forcing load. Damped vibration is associated with energy dissipation in structure in which one part of the energy is transferred into molecular energy in the structural components and another part is dissipated into contact surfaces of components and surrounding objects, such as joints and atmosphere.

The number of independent coordinates needed to describe the displacement pattern of the vibration body is termed the degrees of freedom. Spring, mass and dashpot, arranged as shown in Figure 2.2, can be displaced in vertical direction only; they have one degree of freedom. Spring represents the restoring force, mass the inertia force and dashpot the resisting force of the system being modeled. For free vibration, these forces are in equilibrium when:

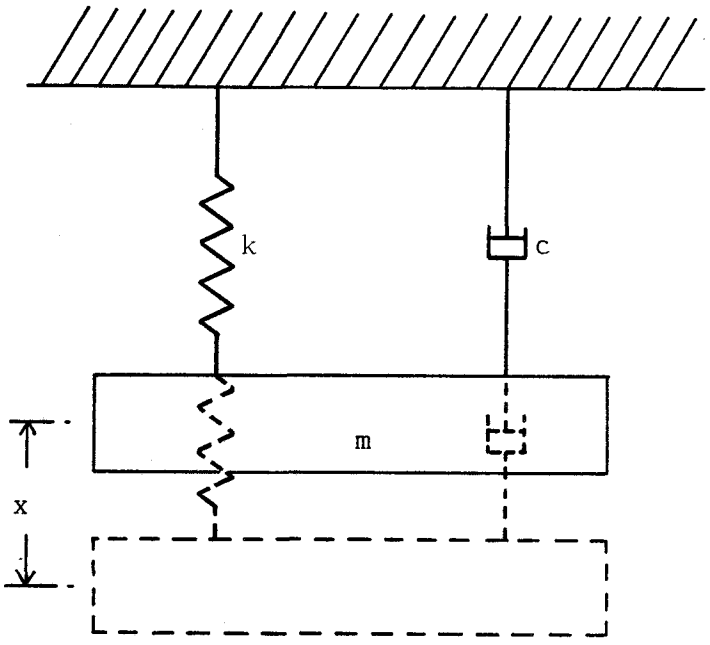

Figure 2.2. Vibration Model for Single Degree-of-Freedom System

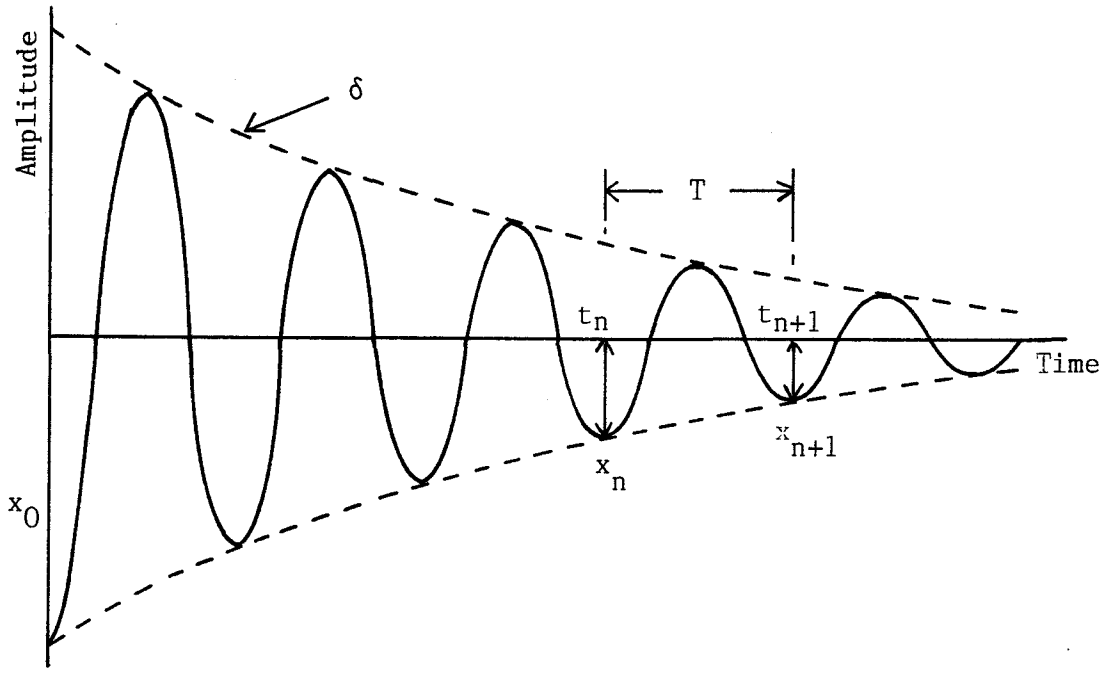

Figure 2.3. Amplitude-Time Relationship from Free Vibration Test

$$m\ddot{x} + c\dot{x} + kx = 0 \quad \ldots\ldots\ldots\ldots\ldots\ldots \quad (2.2)$$

in which m = the mass of the system; k = the spring constant; and c = the viscous damping coefficient. These properties are often expressed as (2.2):

$$c/m = 2\beta, \qquad k/m = \omega_1^2$$

in which ω_1 = fundamental frequency. The substitution of these two expressions into equation (2.2) gives:

$$\ddot{x} + 2\beta\dot{x} + \omega_1^2 x = 0 \quad \ldots\ldots\ldots\ldots\ldots\ldots \quad (2.3)$$

The solution of equation (2.3) takes on a well-known form (2.2):

$$x = \bar{x} \cdot e^{-\lambda\omega_1 t} \sin(\sqrt{1-\lambda^2}\,\omega_1 t + \alpha) \quad \ldots \quad (2.4)$$

in which $\bar{x}$ and α are arbitrary constant depending on how the motion is started; and $\lambda = c/2m\omega_1 = \beta/\omega_1$ is known as damping ratio.

λ can be obtained from free-vibration tests and the assumption of viscous damping. This involves measuring the decrement of decay from the free vibration trace, such as shown in Fig. 2.3. The property measured is known as the logarithmic decrement which is defined as the natural logarithm of the ratio of any two successive amplitudes:

$$\delta = \log_e \frac{x_n}{x_{n+1}} = \log_e \frac{e^{-\lambda\omega_1 t_n}}{e^{-\lambda\omega_1 t_{n+1}}} = \log_e e^{\lambda\omega_1 T} =$$

$$\lambda\omega_1 T \quad \ldots\ldots\ldots\ldots\ldots\ldots \quad (2.5)$$

in which all the symbols are defined in Fig. 2.3. The period of damped vibration is equal to (2.2):

$$T = 2\pi/(\omega_1 \sqrt{1-\lambda^2}) \quad \ldots\ldots\ldots\ldots\ldots\ldots \quad (2.6)$$

Substituting equation (2.6) into equation (2.5) gives:

$$\delta = 2\pi\lambda \; / \; \sqrt{(1-\lambda^2)} \quad \ldots\ldots\ldots\ldots\ldots\ldots \quad (2.7)$$

If λ is a small, then:

$$\delta = 2\pi\lambda \qquad \text{and} \qquad \lambda = \delta / 2\pi \quad \ldots\ldots \quad (2.8)$$

Substituting equation (2.8) into equation (2.5) results in:

$$\lambda = (1/2\pi) \log_e \frac{x_n}{x_{n+1}} \quad \ldots\ldots\ldots\ldots \quad (2.9)$$

Free vibration method is preferred, if the damping ratio is small. In one-nail joints, free vibration test can not be conducted easily [7], which has negated its use in this study.

2.1.4.2. Damping by Static Cyclic Test. This test is commonly used to evaluate damping in laboratory-built systems. It consists of applying to the specimen a static cyclic load which is either load- or deflection-controlled. The resulting load-deflection hysteresis loops are then used to evaluate the energy dissipation and damping of the system.

Jacobsen [13] justified that this test was valid for many applications, but that for pure, highly non-linear restorations or for large values of non-viscous types of damping, the test can become meaningless. The

static cyclic load-slip curves of nailed joints are non-linear, which considerably complicates the exact evaluation of damping. The shape of load-slip hysteresis loops depends on the displacement magnitude as well as on the previous history of loading [14].

A simplified curve from cyclic tests is shown in Figure 2.4. Utilizing such a curve, it is possible to employ the concept of equivalent viscous damping developed by Jacobsen [12]. The total dissipated energy per cycle, ΔW, is represented by the area of the hysteresis loop ABDEA (Figure 2.4). Assuming that all of the curve nonlinearity is due to the damping, and the restoring force to be represented by the linear line EOB, it is then apparent that the area OBCOEFO represents the work capacity, W, per cycle.

Medearis [17, 18] applied the principle of equivalent viscous damping to steady-state forced vibration in his evaluation of damping of plywood diaphragms. The energy dissipated, ΔW, is equal to the work done by the viscous damping force, $-c\dot{x}$, either for half or full cycle. Therefore, knowing the kinetic energies of the system at the time $t = 0$ and $t = T/2$, where T is the period of vibration, the difference between two energies is equal to:

$$\Delta W = KE_{t=0} - KE_{t=T/2} \quad \ldots\ldots\ldots\ldots \quad (2.10)$$

where $KE = m\dot{x}^2/2$

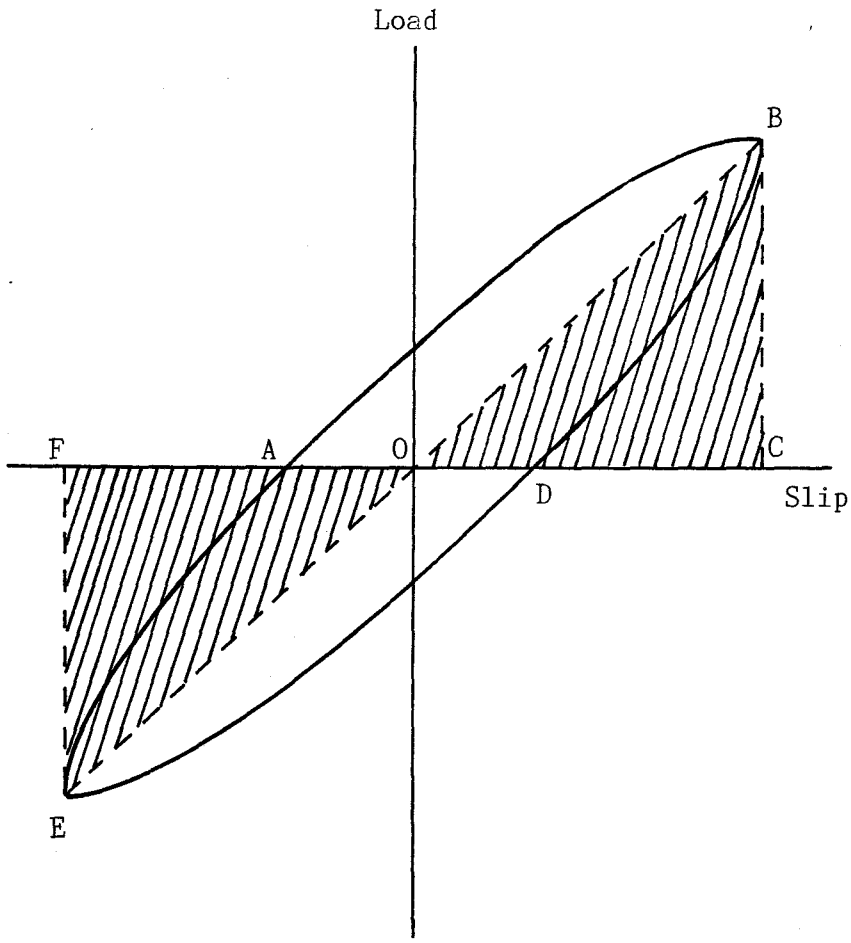

Figure 2.4. Load-slip Curve for Fully Reversed Force

Differentiating equation (2.4) gives:

$$\dot{x} = \sqrt{(1-\lambda^2)}\ \omega_1 \bar{x} e^{-\lambda\omega_1 t} \cos \sqrt{(1-\lambda^2)}\ \omega_1 t - \lambda\ \omega_1 \bar{x} e^{-\lambda\omega_1 t} \sin \sqrt{(1-\lambda^2)}\omega_1 t \quad . \quad . \quad . \quad . \quad (2.11)$$

in which all symbols were identified earlier in the text.

From equation (2.11) follows:

$$\dot{x}_{t=o} = \sqrt{(1-\lambda^2)}\ \omega_1 \bar{x} \quad \text{and} \quad \dot{x}_{t=T/2} = \sqrt{(1-\lambda^2)}\ \bar{x}\omega_1 e^{-\lambda\omega_1 T/2}$$

Substituting these expressions into Equation (2.10), the work done by viscous damping equals:

$$\Delta W = 1/2 m\omega_1^2 \bar{x}^2\ (1-\lambda^2)\ (1-e^{-\lambda\omega_1 T}) \quad . \quad . \quad . \quad . \quad . \quad (2.12)$$

The total work equals the energy of the system at maximum displacement. Because of damping this displacement occurs at a time which is slightly less than the quarter period, T/4, so that the total energy at T/4 is the sum of the kinetic and potential energies:

$$W = K.E._{t=T/4} + P.E._{t=T/4} \quad . \quad . \quad . \quad . \quad . \quad . \quad . \quad (2.13)$$

For t = T/4, we find from equation (2.4):

$$x_{t=T/4} = \bar{x} e^{-\lambda\omega_1 T/4}$$

and from equation (2.11):

$$\dot{x}_{t=T/4} = -\lambda\omega_1 \bar{x} e^{-\lambda\omega_1 T/4}$$

Substituting this expressions into Equation (2.13) gives:

$$W = (1/2)\omega_1^2 m\bar{x}^2 e^{-\lambda\omega_1 T/2} \quad (1 + \lambda^2) \quad . \quad . \quad . \quad . \quad (2.14)$$

which is further substituted into equations (2.12) and (2.14) to give:

$$\Delta W/W = \frac{(\tfrac{1}{2})m\omega_1^2\bar{x}^2(1-\lambda^2)(1-e^{-\lambda\omega_1 T})}{(\tfrac{1}{2})m\omega_1^2\bar{x}^2(1+\lambda^2)\quad e^{-\lambda\omega_1 T/2}}$$

$$= (e^{\lambda\omega_1 T/2} - e^{-\lambda\omega_1 T/2})[(1-\lambda^2)/(1+\lambda^2)] \quad (2.15)$$

Making use of $T = 2\pi/\omega_1\sqrt{1-\lambda^2}$ and of the known relationship [5]

$e^{\alpha} - e^{\alpha} = 2 \sinh \alpha$ gives:

$$\Delta W/W = 2 \sinh (\lambda\pi/\omega_1\sqrt{1-\lambda^2})[(1-\lambda^2)/(1+\lambda^2)] \quad (2.16)$$

For small λ, Equation (2.16) can be simplified by using the known relationship [5] $\sinh x = x + x^3/3! + \ldots + x^{2n+1}/(2n+1)!$ gives:

$$2 \sinh \lambda\pi \;/\sqrt{1-\lambda^2} \simeq 2\pi\lambda$$

and

$$\Delta W/W \simeq 2\pi\lambda \text{ or } \lambda = 1/2\pi\,(\Delta W/W) \quad (2.17)$$

This concept is based on the equivalence of the dissipated work of actual damping force and viscous damping force, $c\dot{x}$, which is proportional to the velocity. The concept of viscous damping is the most accurate at small loads and displacements. The best estimate of the dissipated work can be obtained by taking the average of the area above and below the slip axis (Fig. 2.4).

2.2 Discussion of Pertinent Literature

In the past, much research has been conducted on the strength of nailed joints [3,4,9,10,14,22,28,29]. The evaluation of joint stiffness is of recent origin [29]. This stiffness was initially assumed to be elastic; only recent investigations [10,22] include inelastic stiffness.

Research on damping properties of materials was started almost 200 years ago [30]. Most studies have been concerned with damping properties of specific materials under specific loading condition. Studies on damping of wood are of more recent origin; for maple wood, Kimball and Lovell [15] presented the material damping as a frictional damping. During the past two decades several studies have been performed on damping characteristics of wood material, but they were limited to low-stress range [13]. Damping in wood joints has been evaluated experimentally [17, 18, 24] and attempts have been made to predict damping theoretically [30].

Atherton et al [4] studied the effect on nailed joints of friction in the interface between studs and plywood. At five load levels, he applied four fully reversed loading cycles to one-nail joints. Friction in contact surfaces affected joint response markedly, but Atherton assumed that the friction effect was small in real structures, because green lumber has been commonly used in light-frame wood construction. Subsequent drying

produces gap and reduces friction.

Kaneda [14] made both theoretical and experimental studies of joint damping and stiffness. He investigated damping of single nailed joints and of composite nailed structure. He indicated that the main sources of damping were the friction between frame and sheathing material and the plastic yield of wood in the neighborhood of the nail. His other conclusions are that the energy loss per cycle of loading depends only on the slip but not on the absolute load value, and that the effect of grain direction of the frame member and sheathing panel is appreciable.

Medearis [17, 18] tested eight 8- by 8- foot plywood shear walls to failure with fully reversed tension and compression cycles of loading. Absorption of cyclic energy was calculated as a measure of damping. He found that during any given half cycle the energy absorption was about 60% of the energy at the beginning of the half cycle.

Yeh [30, 31] tested nail joints in double shear under compression loading cycled up to 100 times. He employed prebored nail holes in covering to eliminate nail bearing effect on joint stiffness. He also developed a theoretical model that used the results from tests of one-nailed joint specimen to predict the overall damping of the T-beams made with lumber and

plywood. However, the predicting model correlated poorly with experimental results.

A few attempts have been made to evaluate the effect of damping on loading rate. Polensek [22] tested full-size components, and one nail-joints under several levels of static cyclic loading. Components were also tested under dynamic loading consisting of free, sinusoidal vibration, and simulated seismic vibration. The rate of loading appeared to have a pronounced effect on damping; the damping ratio, from free vibration test was observed to be several times larger than the corresponding ratio from static test. He also indicated that the joint behavior was the main source of the component non-linearity. For one-nail specimens under sinusiodal loading, the loading rate strongly correlated with damping ratio. The ratios at 1.0 hertz were found to be larger than those at 0.1 hertz, which was also characterized by different shape of hysteresis loops. For fully reversed triangular or ramp loading, both loading rate and level, had a significant but small effect on damping ratio.

Chou Chun [7] conducted cyclic load tests on one-nail joints between lumber and plywood to evaluate the effect of wood moisture content on joint properties. The results showed that damping ratio and slip modulus were significantly smaller for joints with the

drying-produced gaps than for those without gap.

Several investigators [9,10,28,29] tried to predict slip moduli theoretically, but theoretical predictions lacked accuracy. Foschi [9,10] developed a model to predict the load-slip relationship for nailed joints between plywood and lumber. His model requires the empirical data on elastic bearing modulus of wood and it predicts the backbone curve for the load-slip relationship.

Wilkinson [28,29] modeled elastic portion of the load-slip relationship. He experimentally evaluated foundation moduli needed to use his model for similar joint members. His studies have limited practical appeal because of the over-simplified assumption of linear behavior.

Testing procedures used for nailed joints vary and no standard methods exist for evaluation of dynamic properties, such as damping. Although some evidence exists [22] on effects of testing speed on damping and stiffness, the existing literature on this topic does not provide reliable solutions. This study is aimed at looking at a few basic questions about the effect of testing speed on the properties of typical nailed joints.

III. MATERIALS AND METHODS

Several experimental techniques, reported by other investigators [7,16,22], were examined for suitability of application to this study. Some techniques were applied directly and others were modified. This chapter covers the description of materials and testing arrangement employed in this study.

3.1. Experimental Design

Table 3.1 characterizes experimental samples used in this study. A total of eight samples were tested in single shear, each representing one-nailed joint between typical framing and sheathing materials. Each sample was tested at different loading rate. The loading functions employed were ramp and sinusiodal functions with much larger rates of loading than those of the American Society for Testing and Materials (ASTM) [2]. Six sinusiodal loading rates that are listed in Table 3.1 correspond to the ranges of fundamental frequencies expected in wood buildings. Testing was aimed at defining the relationship for damping and stiffness between the ASTM loading rate and the rates used in the recent testing [22].

To reduce the variability in specimen properties and to enhance the statistical reliability, the same

Table 3.1. Description of Samples and Loading Types

Sample No. *	Load		Number of Readings per Second			
	Function	Rate or Cycling Frequency	70	100	130	160 (lb.)
1	Ramp	0.15 in./min.	20	10	5	2
2	Ramp	1.5 in./min.	80	50	40	20
3	Sine	1.0 Hz	200	200	200	200
4	Sine	2.5 Hz	250	250	250	250
5	Sine	4.0 Hz	400	400	400	400
6	Sine	7.0 Hz	700	700	700	700
7	Sine	10.0 Hz	900	900	900	900
8	Sine	15.0 Hz	900	900	900	900

* Each sample had 30 replications.

sections of sheathing materials and lumber were used for all samples. Each stud and plywood section was tested 8 times, once for each loading function shown in Table 3.1. Because each sample consisted of 30 replications, a total of 240 specimens was tested.

3.2. Material Selection and Conditioning

3.2.1. Studs

Two hundred forty five sections of Douglas-fir lumber of nominal size of 2- by 4-inches were selected from an unusued portion of the material from a recent study [11]. The studs were kiln dried and stored in a conditioning room at an equilibrium moisture content of about 12%.

The selection of clearwood lumber sections was mainly based on the specific gravity, so that the histogram of the specific gravity of the selected lumber sections matched a previously determined distribution of a Douglas-fir sample [23]. The histogram for MOEs of selected sections was also matched to that of the same Douglas-fir sample [23]. The MOE's of selected sections were obtained from a previous study [11].

After material selection, 13-inch sections were cut from individual pieces. Each section was weighed and measured for volume and moisture content. Moisture

content was measured by a resistant type moisture meter. The volume was adjusted to ovendry base using tabulated shrinkage volume for clearwood [27]. Therefore, the specific gravity reported is based on oven-dry weight.

MOEs used in the selection are those of beams tested on 114-inch span and adjusted to 12% moisture content. Therefore, the local MOE of 13-inch section, used in this study, may differ somewhat from the MOEs used in the selection. However, it is assumed that this had a negligible effect on matching each section with the appropriate histogram.

3.2.2. Sheathing Material

Three 4-by 8-foot sheets of 3/8-inch thickness, three-ply Douglas-fir plywood of sheathing grade, were obtained from a local supplier. Each sheet was first cut into 4-inch by 8-foot strips with face grain oriented parallel to the long axis of the strip. Next, each strip was then cut into 16-inch lengths. All pieces that contained defects, such as knots and gaps between lamination, were discarded.

3.2.3. Nails

The 6d, galvanized, smooth, box nails were used for all specimen. The nails were 2.1 inches long, the average shank diameter was 0.099 inch and head diameter was 0.25 inch. All came from same keg.

Table 3.2. Classes of Probability Density for Modulus of Elasticity and Specific Gravity of Lumber

Specific Gravity		Number of Specimen	Modulus of Elasticity (p.s.i.)	
Class	Probability	30	Class (10^6)	Probability
0.42	0.024	0	1.47	0.02
0.42 - 0.45	0.044	1	1.47 - 1.69	0.05
0.45 - 0.48	0.12	4	1.69 - 1.91	0.20
0.48 - 0.51	0.24	7	1.91 - 2.13	0.19
0.51 - 0.54	0.23	7	2.13 - 2.35	0.14
0.54 - 0.57	0.16	5	2.35 - 2.57	0.09
0.57 - 0.60	0.08	3	2.57 - 2.79	0.136
0.60 - 0.63	0.06	2	2.79 - 3.10	0.07
0.63 - 0.66	0.03	1	3.10 - 3.23	0.08
0.66 - 0.69	0.012	0	3.23 - 3.45	0.024

3.3. Specimen Construction

To enable easier construction the following steps were carried on. Center lines were drawn on the narrow face of each stud section, parallel to the long axis to provide easier alignment of stud and plywood sections. For connecting the sections to the testing apparatus, two 3/8-inch holes were drilled on the center line of narrow face parallel to the wide face 5/8 inch away from the stud end (Fig. 3.1). To assure proper nail placing, nail-penetration sites were marked on the center line of the narrow face of each stud section. To achieve uniform nailing 5/62-inch holes were drilled in each wood and plywood sections at preselected nail locations 2 inches from the end (Fig. 3.1).

A center line was drawn on each sheathing piece parallel to the long side. Then two 3/8-inch holes were drilled 1 and 5/8 inches away from one of the ends (Fig. 3.1). These holes were for the bolts that connected the joint specimen to testing machine. After manufacturing, the specimen were conditioned in the conditioning room at equilibrium moisture content of 12% for about four months.

All specimens had the interface length of 4 inches. They were assembled as follows. The nail was positioned on the predrilled 5/64-inch hole and driven first into

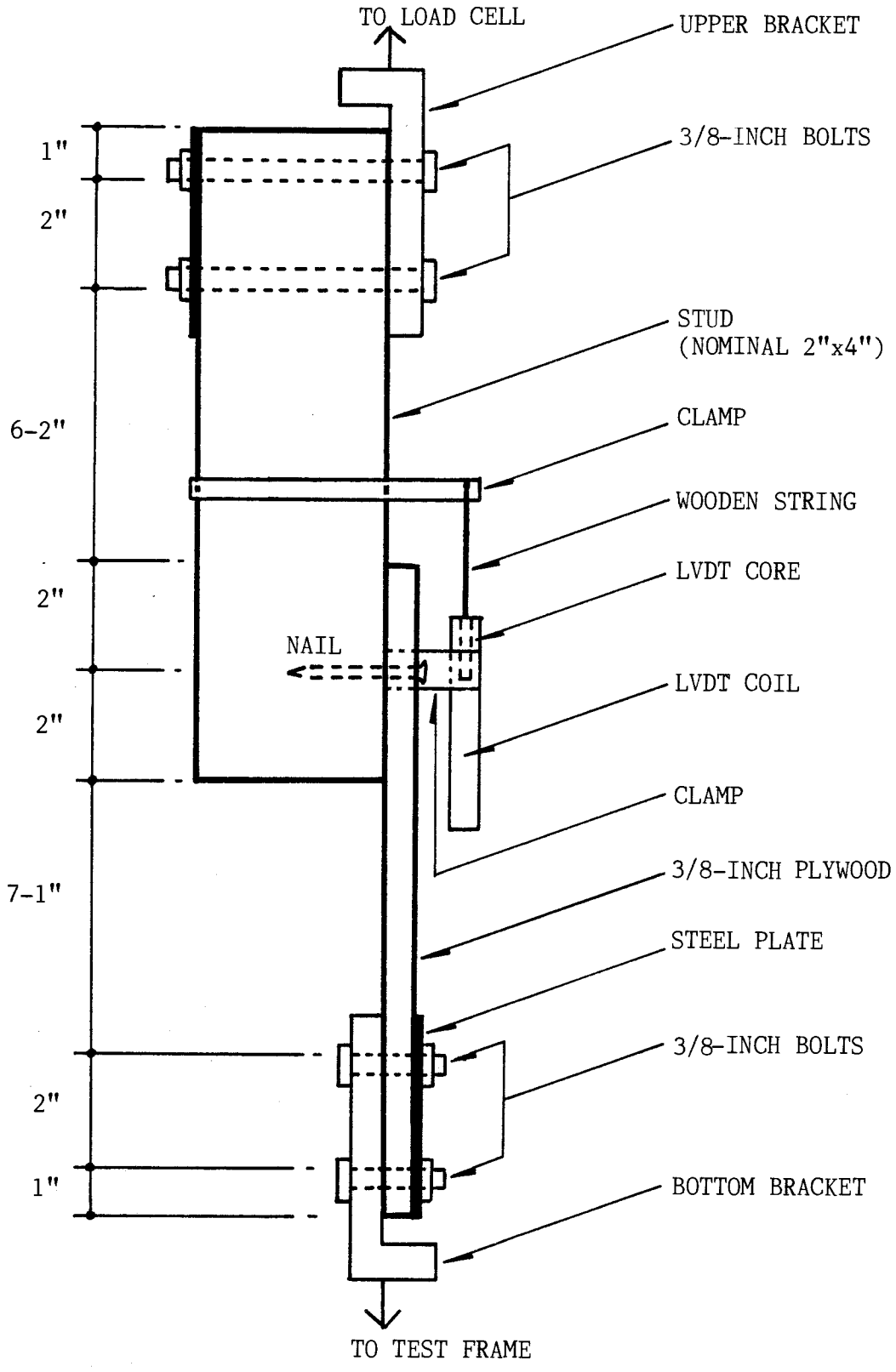

Figure 3.1. Specimen Construction and Testing Arrangement

the plywood, and then into the wood until head was 5/8 inch above the plywood surface. Next, the specimen was placed on the testing machine and the nail pushed in until the top of the head was in the plane of the plywood surface. Next, the specimen was placed on the testing machine and the nail pushed in until the top of the head was in the plane of the plywood surface. The predrilling of nail holes and machine-pushing of nails was carried out to reduce the variability associated with specimen construction. The reduced variability should increase the power of statistical testing.

The specimens were disassembled after testing and 1-inch strip cut off from each plywood section close to the used nail hole. A new specimen was constructed from these plywood and stud section but with a new nail. Then the testing was performed at a different loading rate. After testing and cutting plywood sections twice, the stud ends were cut off in the same way. For each successive specimen construction, the nail sites were moved 1 inch along the center lines of the wood and plywood sections, except when the stud section was attached to the opposite narrow face of the wood section. The interface length between lumber and sheathing of 4 inches was kept constant for all the specimens.

3.4. Testing Arrangement

Whenever possible established procedures were used. Several new details were designed, because the established procedures did not provide all the details needed in this study.

3.4.1. Specimen Mounting

The assembled specimens were mounted to the testing machine by brackets attached to test frame (Fig. 3.1). This arrangement minimized the bending effect, because the applied force acted through the plane that was parallel and very close to the joint interface.

A linear variable differential transducer (LVDT) was used to monitor the slip between the lumber and sheathing, and load cell was used to monitor the applied load. The mounting procedure consisted of first attaching the top bolts through the holes in the upper mounting bracket and through the holes in the lumber piece and steel plate and then tightening the bolt nuts. The LVDT coil part was positioned parallel to the stud length and clamped to the plywood section. The LVDT core was attached to a wooden rod that was clamped to the stud (Fig. 3.1). The rod had an adjustment screw that allowed the core positioning with respect to the coil. After inserting the core into the coil, the bottom bolts were placed through the bracket and the plywood section and

the steel plate and the nut was tightened. Then the adjustment screw was turned until a zero voltage output was read on a voltmeter used in calibration. Finally, the X-Y recorder was positioned at zero for both load and slip.

3.4.2. Loading Functions

All samples were subjected to cyclic loading at four load levels each cycled three times (Figures 3.4 and 3.5 and Table 3.1). Sample No. 1 has a rate of loading (Table 3.1) that corresponds to the ASTM rate [2]. Sample No. 2 has a function used in an earlier investigation aimed at developing data base for damping of most important nailed joints in wood buildings [22]. Other samples have functions expected during earthquake and wind loading. The frequencies of these functions were selected in such a way as to provide the data for the statistical regression analysis.

The rate of sample No. 2 was 1.5 in./min. because the ASTM rate of about 0.15 in./min. was considered too slow and time consuming for efficient testing of large number of specimens under cyclic loading [2]. It is hoped that the results of this study will provide the relations for correcting damping ratios obtained at 1.5 in./min. rate to those expected in earthquakes.

3.4.3. Arrangement for Applying Load Functions

For ramp function, the cycling was applied automatically three times at each load level, but the testing equipment had to be manipulated manually to advance to the next level. The rates and frequencies for sinusoidal functions were too high for a smooth manual change to a higher load level. Therefore, a special testing arrangement was designed (Fig. 3.2) which allowed automatic advancement to the next higher load level.

This arrangement called for adding a sweep/modulation generator. This generator automatically changes the load level by applying the amplitude modulation input as a linear function of programmed input. The syncronous function modulator was designed to compliment the operation of a sweep/modulation generator to control both amplitude and frequency changes in the generator for input to testing machines, such as the one used in this study. Before applying the load, each loading rate and level was checked by the oscilloscope, for its accuracy.

3.4.4. Data Acquisition Arrangement

The slip was measured by an alternative-current LVDT with an accuracy of 0.0001 in. LVDTs are

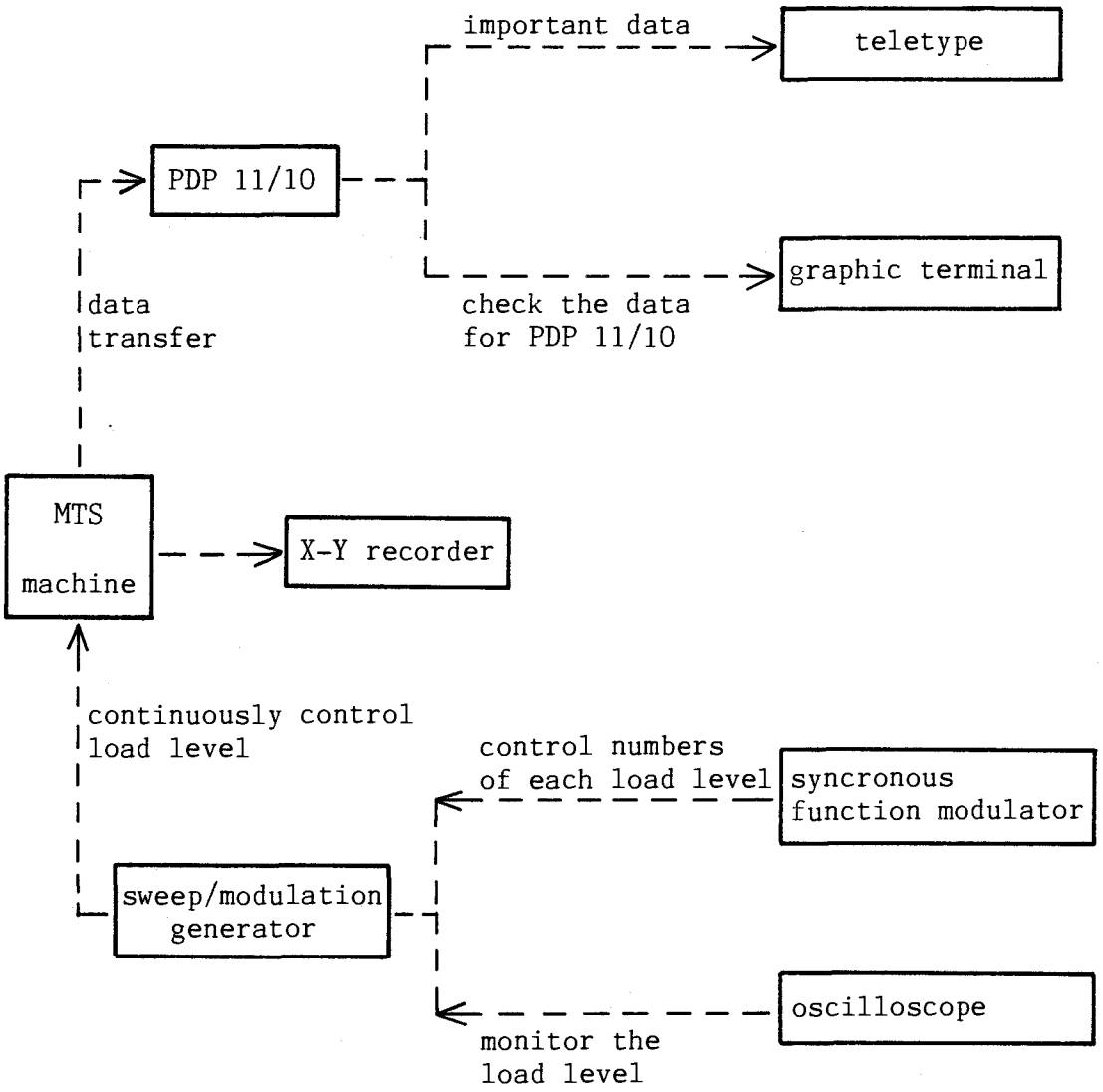

Figure 3.2. Block Diagram for Arrangement of Load Control and Data Acquisition

electromechanical devices which produce a voltage that is proportional to the displacement of the metal core in the coil. By being attached to wood and sheathing, the LVDT monitored the slip or relative displacement between the stud and sheathing.

The load was continuously monitored throughout each test by the load cell up to an accuracy of 0.1 pounds. Load cells are transducers that are excited by the input current and produce a variable voltage that can be calibrated directly in terms of the applied force.

Two data acquisition systems were employed in an arrangement shown in Figs. 3.2 and 3.3. They were a PDP 11/10 microcomputer and an X-Y recorder. Outputs from the LVDT and load cell were recorded on the magnetic tape of the microcomputer. In addition, for sample Nos. 1, 2 and 3, the slip and load signals were also recorded on the X-Y recorder. The data on the X-Y recorder were used to check the accuracy of the information on the magnetic type, as well as the accuracy of damping ratios and slip moduli, computed by the microcomputer.

3.4.5. Testing

To eliminate the effect of moisture-content changes, all tests were conducted in the conditioning

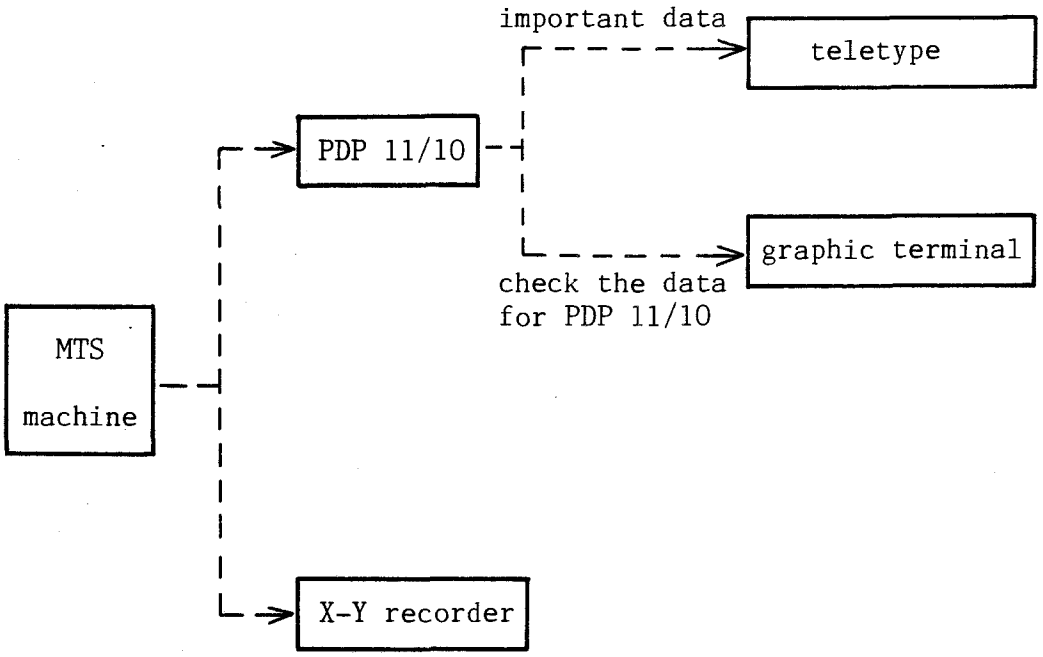

Figure 3.3. Block Diagram Used in Data Acquisition

room maintained at about 12-percent equilibrium moisture content, that is at a constant temperature of 70°F and constant 65% relative humidity.

Specimens were assembled shortly before testing. Sample No. 1 was tested first and then the damping ratios were computed for each load level of each specimens. The specimens were disassembled and reassembled into specimens for sample No. 2. These basic steps were then repeated for each successive sample number.

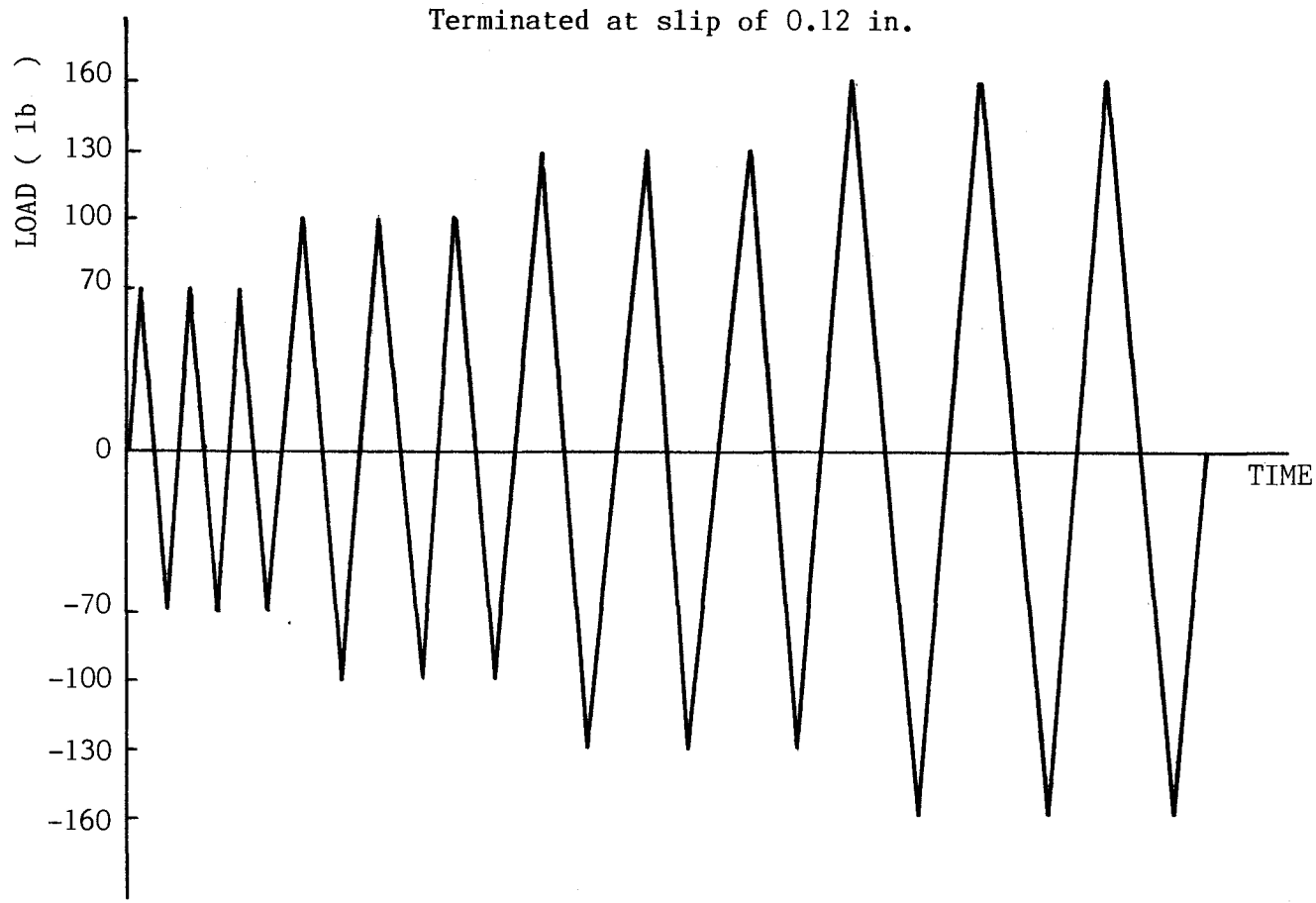

Figure 3.4. Diagram for Ramp Loading

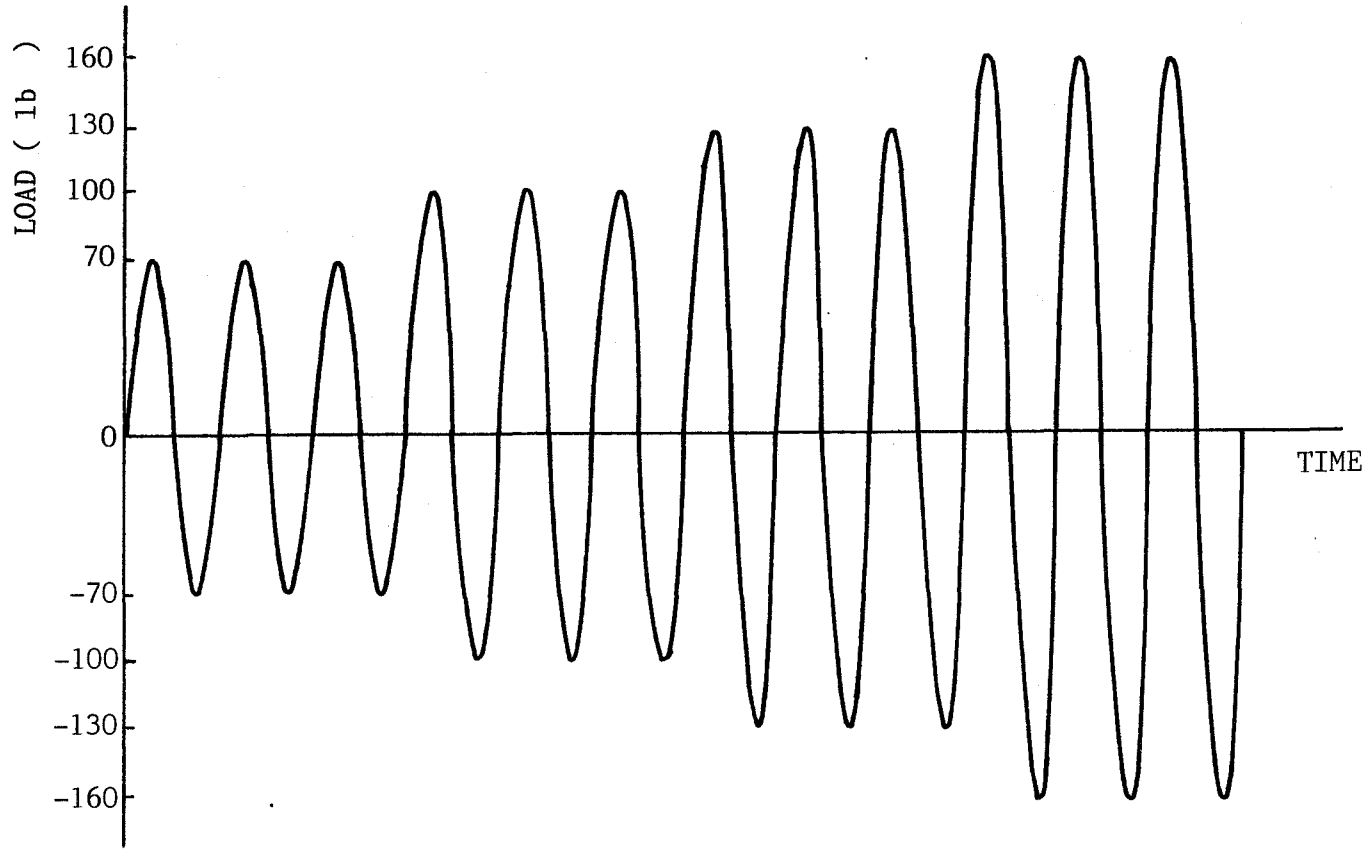

Figure 3.5. Diagram for Sinusoidal Loading

IV. RESULTS AND DISCUSSION

This chapter covers the data analysis, presents the reduced data, and discusses the most important results, all of which are based on the experiments described in Chapter III.

4.1. Reduction of Experimental Data

4.1.1. Data Description

Figs. 4.1, 4.2 and 4.3 illustrate typical load-slip traces recorded directly during testing. These traces are non-linear, especially at higher load, and possesses a considerable damping as indicated by the large hysteresis loops. Some traces are non-symmetrical with respect to the load axis, possibly because the local material properties in lumber and plywood on one side of the nail are different from those on the other side. The slip never returns to zero after complete unloading because of the permanent set that gets progressively larger under increasing loads. Consequently, the behavior of nail joint depends on the previous loading.

The traces that were recorded by microcomputer are shown in Figs. 4.2 and 4.3. The traces, consisting of discrete readings connected by straight lines, are not as smooth as those of X-Y recorder. The smaller the

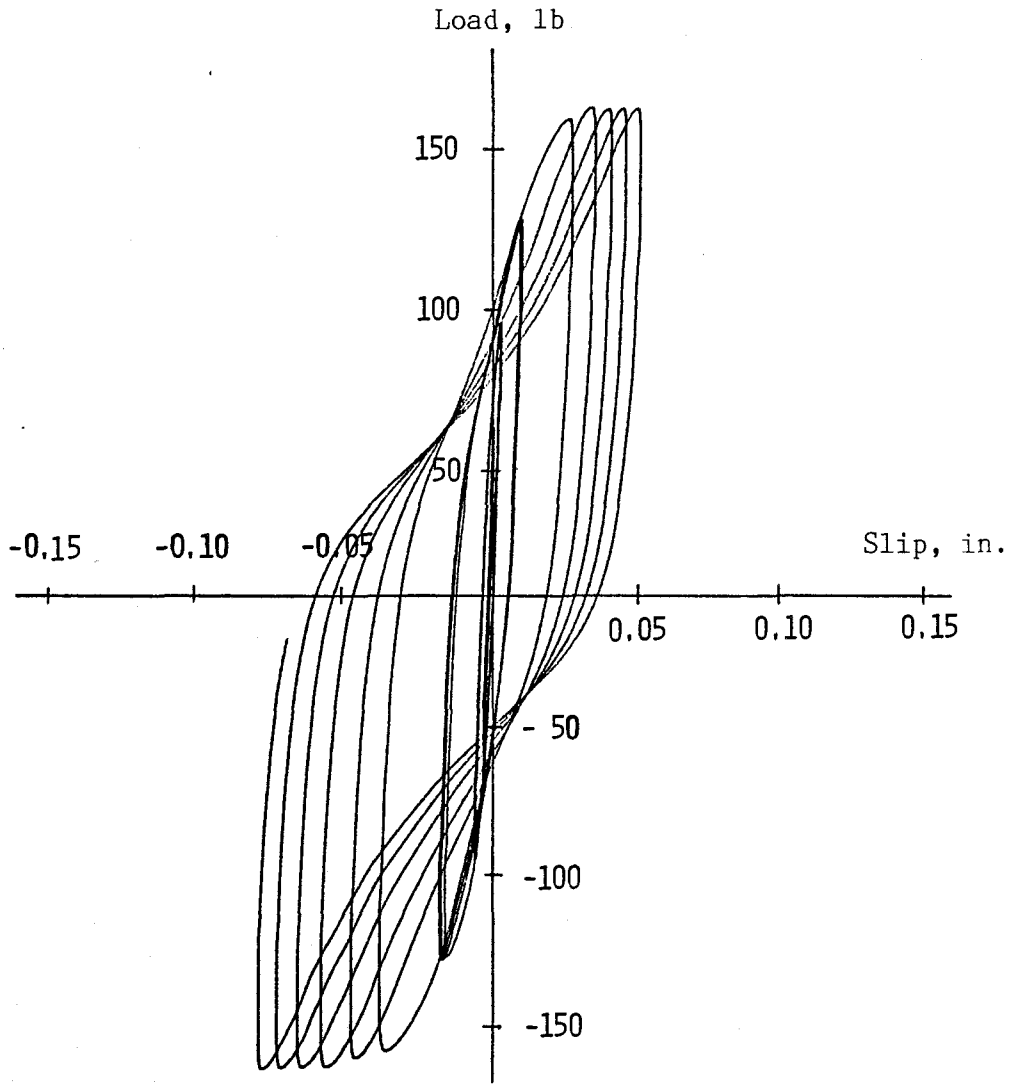

Figure 4.1. A Typical Load-Slip Trace, Obtained by an X-Y Recorder, of Sample No. 3 with 1-Hertz Sine Loading

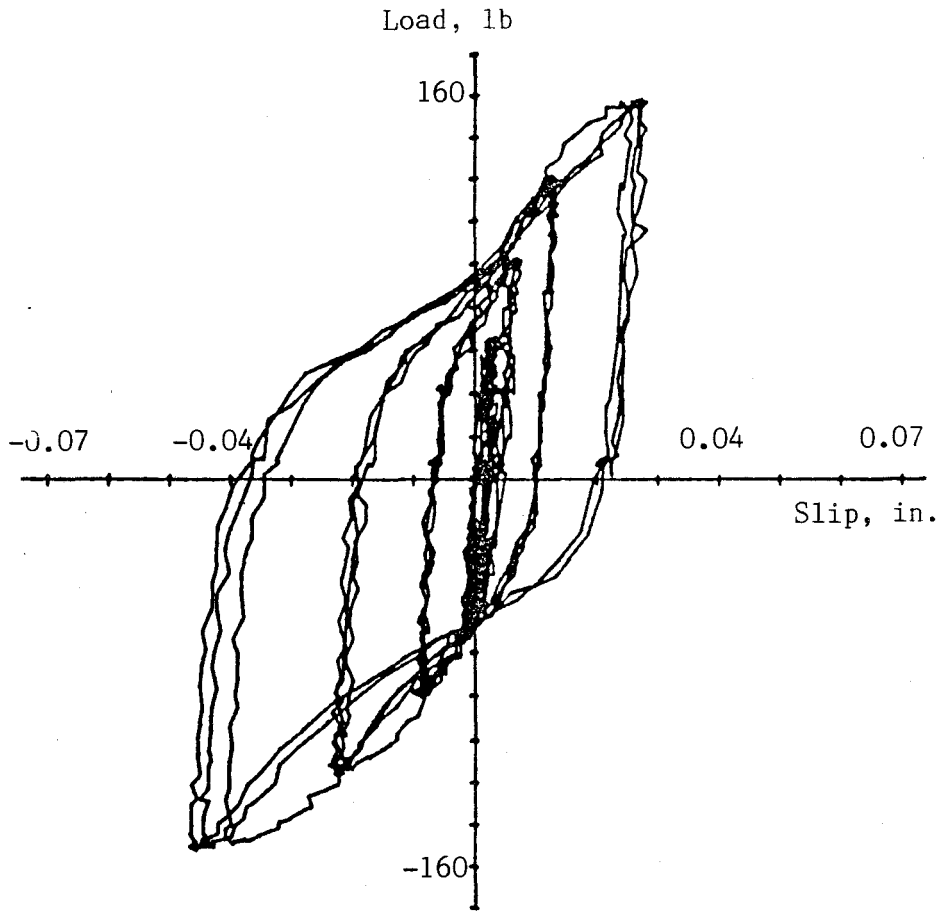

Figure 4.2. A Typical Load-Slip Trace, Obtained by a Data Acquisition System, of Sample No. 3 with 1-Hertz Sine Loading

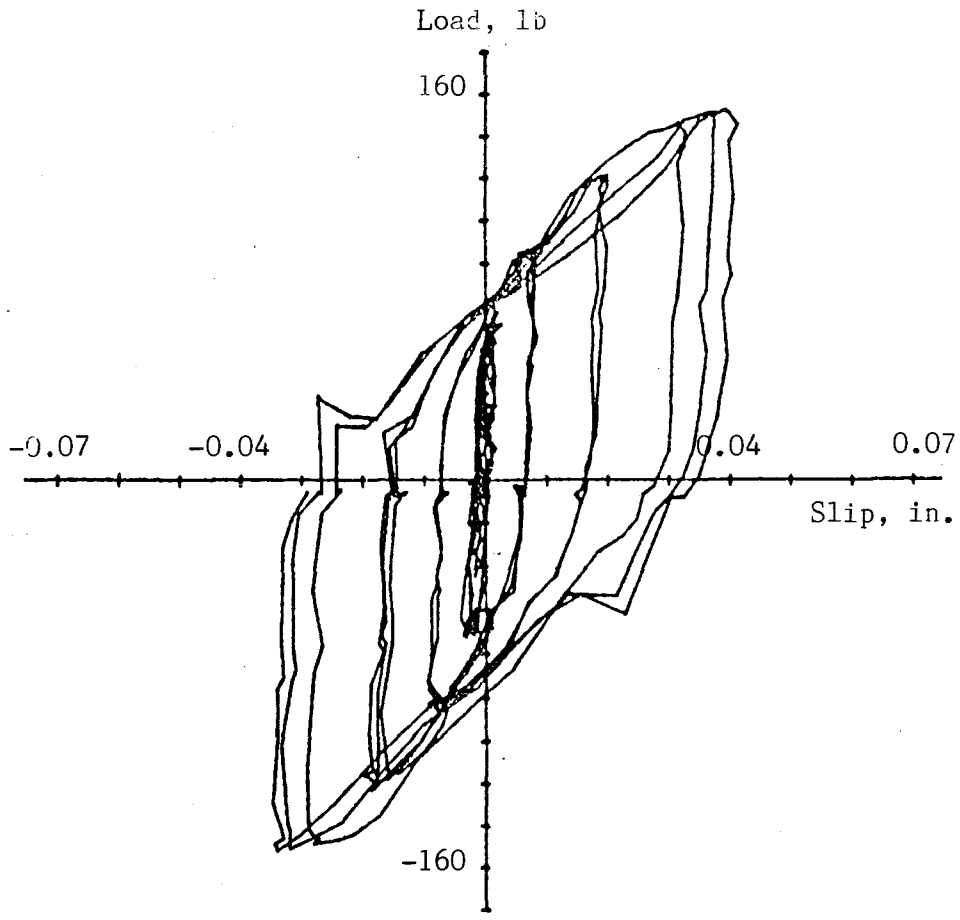

Figure 4.3. A Typical Load-Slip Trace, Obtained by a Data Acquisition System, of Sample No. 7 with 10-Hertz Sine Loading

density of reading points, the smoother the traces. Because the maximum available density was used for each testing speed, smoother traces could not be obtained with the data acquisition system used. It is assumed that the trace roughness has a negligible effect on the size of the areas representing the absorbed energy, because the discrete points above the trace, if smoothed, are balanced by those below the trace.

The hysteretic loops get wider under increased load levels. At 70-lb, the loops are very narrow and loading and unloading traces almost coincide often. Therefore, especially several rough traces at high testing rates produced no meaningful energy areas and were eliminated from the data analysis (Table 4.1). Trace roughness at high load levels and problems with specimen manufacture and testing further reduced the number traces used in data analysis (Table 4.1).

4.1.2. Procedure for Data Reduction

Among the three cycling loops at each load level, the second was not directly affected by the cycling at the lower and higher load. Therefore, the second loop was used to evaluate the joint damping and stiffness. Damping ratios were determined by equation 2.17 in which ΔW and W were evaluated from areas under traces as defined in Figs. 2.4 and 4.4. The evaluation was aimed

Table 4.1. Number of Useful Traces

Loading Rate and Cycling Frequency	No. of Traces* Evaluated at Load Levels			
	70-lb	100-lb	130-lb	160-lb
0.15 in./min.	16	20	20	20
1.5 in./min.	18	23	23	23
1.0 Hz	16	24	24	24
2.5 Hz	8	21	21	21
4.0 Hz	17	21	21	21
7.0 Hz	11	20	20	20
10.0 Hz	15	19	19	19
15.0 Hz	12	16	16	16

* The target was 25 specimens.

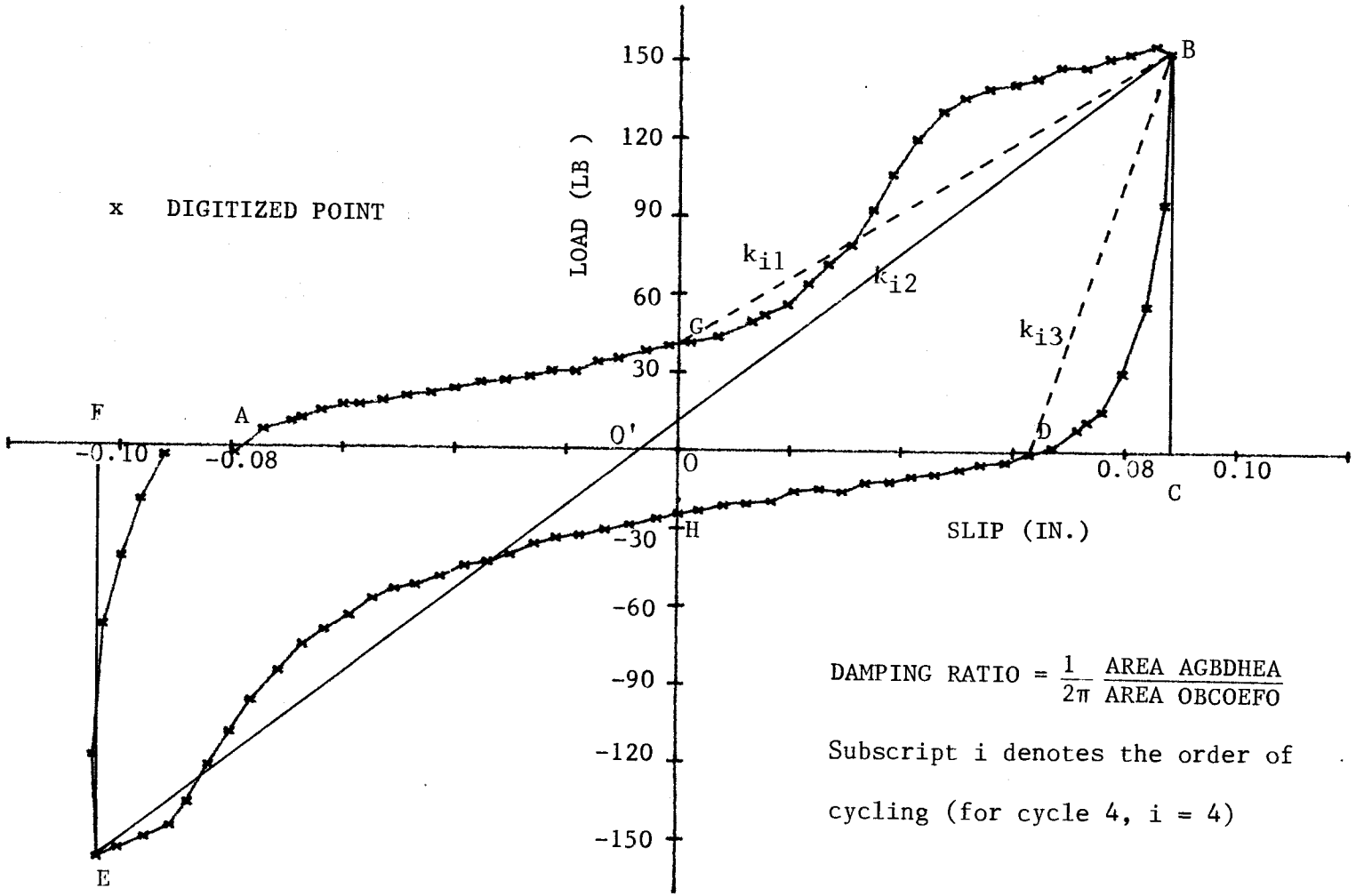

Figure 4.4. A Typical Digitized Load-slip Trace

at generating the following variables: total dissipated energy per loop (Area AGBDHEA in Fig. 4.4), total work capacity per loop (Area O'BCO'EFO' in Fig. 4.4), and damping ratio (Eq. 2.17). The areas were calculated by microcomputer from the test data stored on floppy disks. The initial step consisted of identifying points such as A, G, B, D, H, E (Fig. 4.4), which was followed by selecting a new origin (O') as the middle between the slip at points B and C. This origin was then used to calculate the area of triangle O'BC for work capacity defined by the area O'BC. The area AGBDA of the corresponding dissipated energy was computed by accumulating the trapezoidal areas between the two adjacent slip coordinates.

Other variables evaluated were characteristic points on each load versus slip traces, which were used to define the joint stiffness at each load level. In Fig. 4.4, these points are G,B,D, and O'. They were selected at the intersection of the trace with both coordinate axes and at extreme loads for each cycle. Straight lines through these points linearly approximate the load versus slip relations for each load level used in this study.

The load and slip traces from X-Y recorder were first digitized by a microcomputer-controlled digitizer. The information was then processed in the same way as

that collected by the PDP 11/10 microcomputer system (Appendix A). The values, available energy, dissipated energy, damping ratio and coordinating points identifying stiffness, were then transferred to a large central computer for a statistical analysis.

4.1.3. Statistical Analysis

A standard computerized program, SPSS [20], was used for most of the statistical analysis. Individual and combined effect of loading rate and load level on damping and stiffness variables were evaluated by another package called ANOVA [20].

4.2. Relation Between Damping Ratio and Loading Rate

Table 4.2 lists the means and standard deviation of the dissipated energy, work capacity and damping ratio. These data were analyzed by statistical package ANOVA. First, two-factor analysis was conducted to determine if damping ratio, dissipated energy and work capacity are affected by the load level (LL) and loading rate (LR). The values for the variance ratio, F, that is for the ratio of explained variance (the variance between the samples) and unexplained variance (the variance within samples) were used to identify this effect (Table 4.3). If the critical significant level, α is less than 0.05, the effect is significant. The

Table 4.2. Dissipated Energy, Work Capacity and Damping Ratio

Loading Rate	Load Level	ENERGY (in.-lb)				Damping Ratio	
		Work Capacity		Dissipated Energy			
		M*	SD**	M	SD	M	SD
0.15 in./min.	70	0.455	0.293	0.888	0.448	0.315	0.051
	100	1.749	0.674	2.484	0.793	0.233	0.045
	130	4.209	1.656	5.077	1.699	0.200	0.036
	160	10.770	4.683	12.410	4.644	0.189	0.026
1.5 in./min.	70	0.644	0.274	1.026	0.310	0.263	0.061
	100	1.768	0.618	2.164	0.555	0.205	0.047
	130	3.573	1.631	4.025	1.081	0.181	0.039
	160	9.989	5.380	10.681	4.961	0.181	0.031
1.0 Hz	70	0.341	0.262	0.666	0.600	0.287	0.077
	100	1.181	0.677	2.255	1.347	0.307	0.039
	130	3.222	1.628	6.099	3.016	0.307	0.035
	160	9.395	5.901	18.047	11.003	0.310	0.021
2.5 Hz	70	0.215	0.157	0.447	0.313	0.334	0.040
	100	0.774	0.365	1.552	0.734	0.319	0.038
	130	2.215	0.736	4.176	1.165	0.305	0.028
	160	5.349	1.818	9.693	2.995	0.292	0.022
4.0 Hz	70	0.287	0.142	0.603	0.291	0.338	0.054
	100	1.212	0.499	2.327	0.896	0.312	0.040
	130	3.221	1.190	5.651	1.795	0.288	0.034
	160	7.767	2.792	13.155	3.857	0.278	0.028
7.0 Hz	70	0.162	0.086	0.354	0.208	0.340	0.088
	100	0.896	0.332	1.753	0.659	0.313	0.024
	130	2.514	0.748	4.404	1.074	0.284	0.927
	160	5.779	1.625	9.319	1.855	0.262	0.025
10.0 Hz	70	0.307	0.119	0.867	0.523	0.313	0.040
	100	1.073	0.325	2.317	0.618	0.291	0.034
	130	2.644	0.539	4.400	0.821	0.259	0.029
	160	5.689	1.293	7.469	0.845	0.242	0.028
15.0 Hz	70	0.387	0.171	0.605	0.239	0.323	0.061
	100	1.305	0.457	1.925	0.502	0.291	0.043
	130	2.863	0.718	4.244	0.717	0.250	0.040
	160	5.314	1.158	8.478	1.292	0.230	0.038

* M : Mean ** SD : Standard Deviation

Table 4.3. Analysis of Variance for Effects of Load Levels and Loading Rates on Damping Variables

Variable*	Degree of Freedom	Source of Variation	F-statistic	
			Computed**	Limit
Dissipated Energy (in.xlb.)	3	Load Level	403.24	2.62
	7	Loading Rate	12.43	2.03
	21	Interaction	6.09	1.58
Work Capacity (in.xlb.)	3	Load Level	375.69	2.62
	7	Loading Rate	13.85	2.03
	21	Interaction	4.44	1.58
Damping Ratio	3	Load Level	68.57	2.62
	7	Loading Rate	75.15	2.03
	21	Interaction	4.49	1.58

* Sample sizes identified in Table 4.1

** Significant at 0.05-level if computed F > limit F

individual effect of load level and loading rate were found to be significant in all cases (Table 4.3).

In addition to individual effects, the interaction between the load level and loading rate was examined at $\alpha = 0.05$. The results show that a significant two-way interaction exists between the load level and loading rate for all three dependent variables: dissipated energy, work capacity, and damping ratio (Table 4.3). Because the interaction between the two effects was significant for all the load levels, the analysis was conducted separately at each level. Thus, the analysis of load-level effects on the three dependent variables was conducted individually for each loading rate. A strong correlation also was found between the damping ratio and load level (Table 4.4). The corresponding computed F-values are greater than F-value limits at the 0.05 level except for the damping ratio at 1.0 Hz. This shows that the load level influences the damping ratio at all loading rates except for 1.0 Hz. Furthermore, the results show that the load level influences dissipated energy and work capacity at all loading rates.

An examination of data in Table 4.2 indicates an increase in dissipated energy and work capacity with an increase in load level. Logically, the energies get larger at higher load and slip. Consequently, the same effect is observed for damping ratio and loading rate (Table 4.5).

Table 4.4. Analysis of Variance for Effect of Load Levels on Damping Variables

Loading Rate	Sample Sizes	F-statistic			
		Computed*			Limit
		Damping Ratio	Work Capacity (inxlb)	Dissipated Energy(inxlb)	
0.15 in/min	76	35.22	60.27	74.10	2.74
1.5 in/min	87	14.50	44.77	58.84	2.72
1.0 Hz	88	1.08	35.77	37.95	2.72
2.5 Hz	71	4.49	77.44	90.30	2.75
4.0 Hz	80	8.59	88.85	123.37	2.73
7.0 Hz	71	115.49	8.94	187.12	2.75
10.0 Hz	72	16.58	188.25	323.39	2.74
15.0 Hz	60	12.13	122.07	226.17	2.78

* Significant at 0.05-level if computed F > limit F

Table 4.5. Analysis of Variance for Effect of Loading Rates on Damping Variables

Load Level	Sample Sizes	F-statistic			
		Computed*			Limit
		Damping Ratio	Work Capacity (inxlb)	Dissipated Energy(inxlb)	
70 lb.	113	2.89	8.93	4.54	2.10
100 lb.	164	24.72	10.18	3.11	2.07
130 lb.	164	42.59	5.56	4.79	2.07
160 lb.	164	64.51	7.53	8.85	2.07

* Significant at 0.05-level if computed F > limit F

In summary, both, dissipated energy and work capacity were found to vary with changes in loading rate. This variation is interrelated, so that the amount of changes from one level to the next is not the same. Consequently, the loading rates also influence the damping ratio.

The data in Table 4.2 indicate that the damping ratio changes more at slower and less at faster loading rates. To determine which adjacent rates affect the damping ratio significantly, T-tests also were conducted at $\alpha = 0.05$. The results show that the damping ratios are significantly different between the adjacent low rates, but not so at the high rates. (Table 4.6, Fig. 4.5, Appendices B and C).

The relation between the load and the dissipated energy, work capacity and damping ratio were also investigated. The ramp loading rates were converted into frequencies to have them expressed by the same variable for all samples. The converted frequencies somewhat varied from specimen to specimen and from load level to load level, because the frequency of the load ramp rate changed with specimen stiffness and nonlinearity. The results for all eight rates were then subjected to linear regression analysis for the following model:

$$Y = A + B \times LL + C \times (LR)^{-D} \quad . \quad . \quad . \quad . \quad . \quad . \quad . \quad (4.1)$$

Table 4.6. T-Test for Damping Ratios and Loading Rates

Loading Rate*	T-statistic**	Loading Rate						
		0.15 in/min	1.5 in/min	1.0 Hz	2.5 Hz	4.0 Hz	7.0 Hz	10.0 Hz
1.5 in/min	C L	2.80 1.97						
1.0 Hz	C L	8.79 1.97	13.36 1.97					
2.5 Hz	C L	9.37 1.98	14.75 1.97	0.72 1.97				
4.0 Hz	C L	8.35 1.98	12.71 1.97	0.30 1.97	1.02 1.97			
7.0 Hz	C L	6.92 1.98	10.64 1.97	1.25 1.97	1.92 1.98	0.96 1.97		
10.0 Hz	C L	5.14 1.98	9.12 1.97	4.41 1.97	5.42 1.98	3.97 1.97	2.58 1.98	
15.0 Hz	C L	4.00 1.98	7.10 1.98	3.92 1.98	4.63 1.98	3.60 1.98	2.55 1.98	0.43 1.98

* Sample sizes identified in Table 4.1

** C = Computed T-statistic

L = Limit T-statistic at 0.05-level

Significant at 0.05-level if C > L

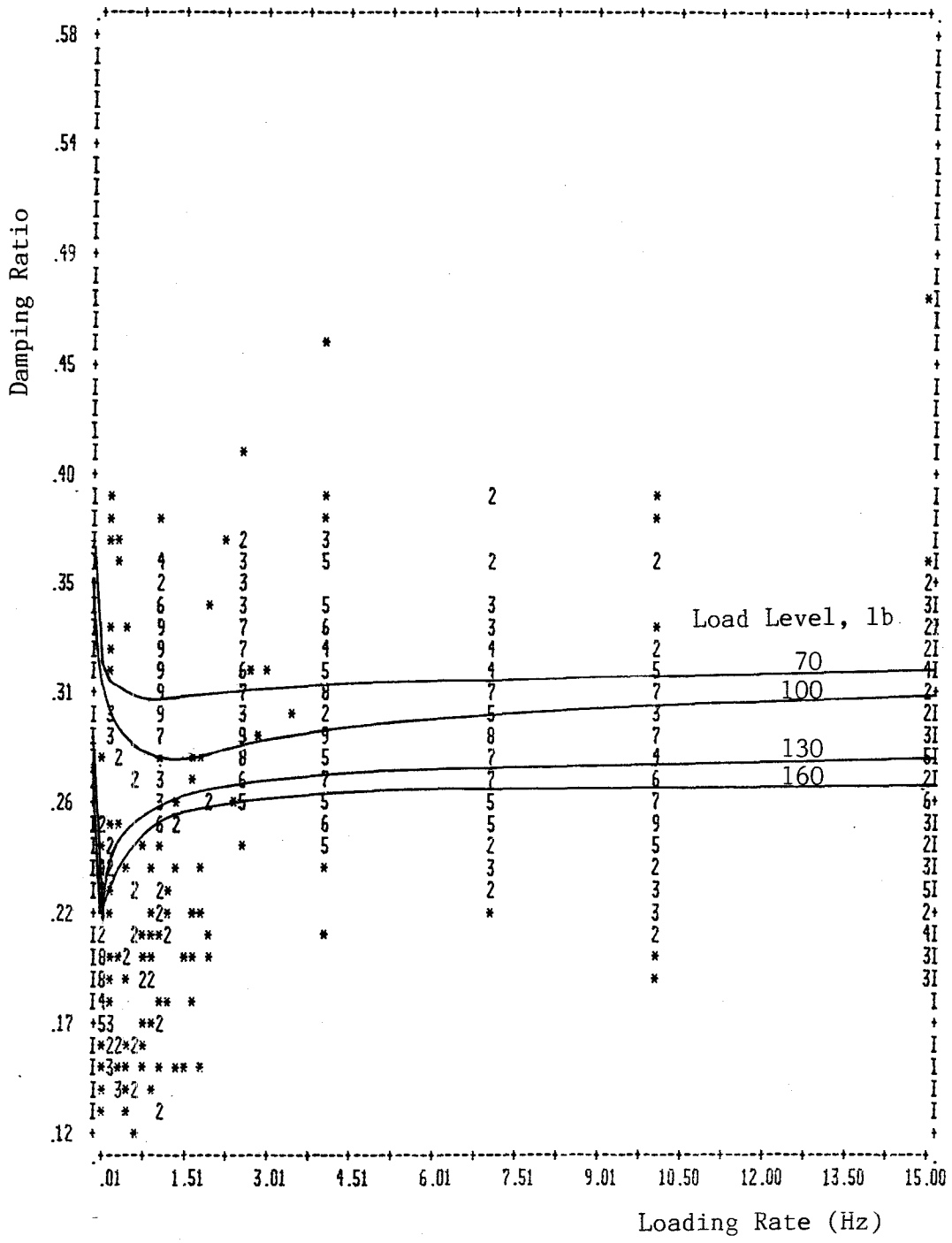

Figure 4.5. Relationship between Damping Ratio and Loading Rates

where A, B and C = regression constant, LL = load level (lb) and LR = frequency associated with test loading (Hz).

Table 4.7 lists the regression constants and correlation coefficients, r. The values of r for work capacity and dissipated energy are above 0.74, that is the value associated with acceptable correlation between modulus of elasticity and modulus of rupture for lumber. However, the values of r in predicting damping ratio are smaller, which means that the testing in this study has not revealed a strong correlation between damping ratio and load level and loading rate.

Additional study included the relation between the individual loading rates and damping ratio. The results show strong correlation at high load level and poor correlation at low load level. (Fig. 4.5).

4.3. Relation Between Stiffness and Loading Rate

The analysis of variance at α = 0.05 was also performed to determine if joint stiffness is affected by loading rate and load level. The stiffness was expressed by the secant slip moduli, k_{ij}, which were defined by the slopes of lines connecting points B-G, B-O' and B-D (Fig. 4.4). Table 4.8 lists the means and standard deviation of these slip moduli. The standard deviation of experimental data is large at 70 lb load level. It is likely that the sample size was too small

Table 4.7. Regression Equations Relating Joint Properties and the Effect of Load Level and Loading Rate

Dependent Variable	Regression Equation: $Y = A + B(LL) + C(LR)^{-D}$				r
Y*	A	B	C	D	
DR	0.386	-0.583E-3	-0.048	0.25	0.517
TOWC	-5.216	0.070	0.003	2.00	0.781
TODC	-7.938	0.109	0.463E-5	3.50	0.745

* DR : Damping Ratio

TOWC : Total Work Capacity per Loop (in.-lb)

TODC : Total Dissipated Energy per Loop (in.-lb)

LL : Load Level (lb)

LR : Loading Rate (Hz)

Table 4.8. Statistics of Slip Moduli for Samples Investigated

Loading Rate \ Statistics		Stiffness Moduli in 1000 lbs /in. for Reversal Levels											
		k_{11}	k_{12}	k_{13}	k_{21}	k_{22}	k_{23}	k_{31}	k_{32}	k_{33}	k_{41}	k_{42}	k_{43}
0.15	M	4.44	12.28	115.87	3.66	6.38	41.88	3.03	4.54	19.86	2.03	2.77	15.49
(in./min.)	SD	2.04	6.59	83.01	0.97	1.92	36.92	0.77	1.42	9.06	0.66	0.10	12.79
1.50	M	4.95	9.67	112.08	4.57	6.90	34.98	3.89	5.35	18.16	2.66	3.50	13.77
(in./min.)	SD	1.54	4.34	110.33	1.08	2.45	43.94	1.14	2.22	10.60	1.37	2.07	8.16
1.0 Hz	M	13.94	20.41	80.26	5.93	12.80	51.65	3.76	6.97	34.26	2.63	3.99	23.86
	SD	13.91	12.95	55.50	3.48	8.83	27.84	1.30	3.70	20.26	1.10	2.24	14.87
2.5 Hz	M	11.18	22.26	119.74	7.06	14.13	115.37	4.51	8.39	47.20	3.60	5.42	28.31
	SD	11.30	11.79	78.16	4.39	6.14	100.05	1.16	2.82	36.10	0.86	1.93	11.65
4.0 Hz	M	12.75	20.61	86.12	4.78	10.79	97.51	6.89	6.49	44.15	2.51	4.07	29.63
	SD	10.61	13.56	60.05	3.84	8.70	113.38	17.28	3.62	43.40	1.10	2.10	21.22
7.0 Hz	M	13.55	32.65	111.35	5.16	11.99	113.25	3.85	7.51	45.04	2.95	4.80	28.62
	SD	21.46	25.90	62.61	1.74	4.47	111.54	0.77	2.10	26.16	0.64	1.32	12.47
10.0 Hz	M	8.37	18.81	122.13	5.28	10.55	66.13	3.62	6.83	39.50	2.95	4.85	30.81
	SD	6.50	6.40	94.49	2.81	3.00	41.84	0.57	1.34	20.62	0.54	1.12	12.42
15.0 Hz	M	5.73	17.12	108.39	5.28	8.83	97.70	3.69	6.31	46.26	3.24	4.98	28.78
	SD	2.91	9.41	83.72	5.36	3.18	108.57	0.78	1.85	27.91	0.75	1.33	17.87

and natural variation too large at 70 lb level.

The results in Table 4.9 show that these moduli depend on both, load level and loading rate. Furthermore, the effect of level and rate is interdependent. As expected, loading rate and load level are strongly correlated to slip moduli, but the effect of loading rate is much weaker. Thus, slip moduli change mostly with level and somewhat loading rate. However, effects of load level and loading rate are not additive.

The statistics in Table 4.10 show that a strong correlation exists between the slip moduli and loading rate. The computed F-statistics, which are greater than F-value limits at $\alpha = 0.05$ for all moduli but k_{21}, k_{31}, and k_{13}, indicate that the loading influences all the slip moduli except k_{21}, k_{31}, and k_{13}. The load level influences the slip moduli except k_{i1} at 15.0 Hz (Table 4.11). This indicates that, for all loading functions investigated, the loading rate has negligible effect on slip moduli k_{i1} and k_{i3}. For this reason, no regression equations were developed to correct the joint stiffness for k_{i1} and k_{i3} to account for the variation in the load function.

Table 4.12 lists the mean and standard deviation of total slip. The load level and loading rate appear to depend on each other (Table 4.8). The computed F-statistics are greater than F-value limits at $\alpha = 0.05$,

Table 4.9 Analysis of Variance for Effect of Load Levels and Loading Rates on Joint Slip and Stiffness

Variable		Source of Variation	Degree of Freedom	F-statistic	
Description	Symbol			Computed*	Limit
Total Slip		Load Level	3	270.10	2.62
		Loading Rate	7	15.92	2.03
		Interaction	21	3.49	1.58
Modulus	k_{i1}**	Load Level	3	29.81	2.62
		Loading Rate	7	3.23	2.03
		Interaction	21	1.86	1.58
Modulus	k_{i2}	Load Level	3	133.08	2.62
		Loading Rate	7	10.95	2.03
		Interaction	21	3.66	1.58
Modulus	k_{i3}	Load Level	3	61.04	2.62
		Loading Rate	7	4.44	2.03
		Interaction	21	1.62	1.58

* Significant at 0.05 level if computed F > limit F

** Subscript i denotes the order of load level (i = 1, 2, 3, 4 for 70-lb, 100-lb, 130-lb and 160-lb level, respectively)

Table 4.10. Analysis of Variance for Effects of Loading Rates on Slip Modulus and Total Slip

Load Level	Sample Size	F-statistic				
		Computed*				Limit
		Slip Modulus			Total Slip	
		k_{i1}**	k_{i2}	k_{i3}		
70 lb.	113	2.26	4.31	0.54	7.52	2.10
100 lb.	164	1.99	5.08	3.51	8.94	2.07
130 lb.	164	0.73	4.29	4.11	6.15	2.07
160 lb.	164	5.31	5.11	4.56	7.22	2.07

* Significant at 0.05 level if computed F > limit F

** Subscript i denotes the order of load level (i = 1, 2, 3, 4 for 70-lb, 100-lb, 130-lb and 160-lb level, respectively)

Table 4.11. Analysis of Variance for Effect of Load Level on Slip Moduli and Total Slip

Loading Rate	Sample Size	F-statistic				
		Computed*				Limit
		Slip Modulus			Total Slip	
		k_{i1}**	k_{i2}	k_{i3}		
0.15 in/min	76	13.64	27.15	19.82	38.24	2.74
1.5 in/min	87	13.25	17.37	13.19	33.44	2.72
1.0 Hz	88	12.05	17.53	12.27	28.22	2.72
2.5 Hz	71	6.77	23.05	9.07	52.59	2.75
4.0 Hz	80	3.33	15.40	4.55	64.42	2.73
7.0 Hz	71	4.29	19.01	7.88	78.39	2.75
10.0 Hz	72	8.73	53.32	11.22	125.26	2.74
15.0 Hz	60	2.18	18.02	4.55	65.37	2.78

* Significant at 0.05 level if computed F > limit F

** Subscript i denotes the order of load level (i = 1, 2, 3, 4 for 70-lb, 100-lb, 130-lb and 160-lb level, respectively)

Table 4.12. Statistics for Total Slip Expressed in Inches

Loading Rate	Load Level							
	70 lbs		100 lbs		130 lbs		160 lbs	
	Mean	SD	Mean	SD	Mean	SD	Mean	SD
0.15 in./min.	0.0142	0.0068	0.0351	0.0139	0.0643	0.0252	0.1385	0.0682
1.5 in./min.	0.0182	0.0077	0.0341	0.0120	0.0573	0.0227	0.1269	0.0702
1.0 Hz	0.0101	0.0075	0.0230	0.0133	0.0486	0.0244	0.1150	0.0734
2.5 Hz	0.0073	0.0055	0.0163	0.0078	0.0345	0.0115	0.0667	0.0230
4.0 Hz	0.0089	0.0042	0.0243	0.0099	0.0490	0.0180	0.0961	0.0354
7.0 Hz	0.0054	0.0028	0.0185	0.0071	0.0383	0.0117	0.0725	0.0213
10.0 Hz	0.0085	0.0033	0.0209	0.0059	0.0400	0.0077	0.0706	0.0169
15.0 Hz	0.0112	0.0055	0.0259	0.0093	0.0443	0.0117	0.0676	0.0156

which indicates that the load level influences the total slip (Table 4.11). The analysis also shows that the loading rates influence the total slip (Table 4.10).

The final investigation was concerned with the relation between load functions, total slip and slip modulus, k_{i2}. It consisted of performing the linear regression analysis for following model:

$$Y = A + B \times LL + C \times (LR)^{-D} \quad . \quad . \quad . \quad . \quad . \quad . \quad . \quad . \quad (4.2)$$

Where A, B, C and D = regression constant; LL = load level (lb); and LR = loading rate expressed as a frequency of loading function (Hz).

Table 4.13 shows resulting regression constants and correlation coefficients. The total slip is highly correlated to the loading rate and load level. An exception is slip modulus, k_{i2}, which shows a weak correlation. Therefore, testing in this study has revealed a strong correlation between load functions and all the slip moduli except modulus k_{i2}.

Table 4.13 Regression Eguations Relating Joint-Slip Properties to Load Level and Loading Rate

Dependent Variable	Regression Equation: $Y = A + B(LL) + C(LR)^{-D}$				r
Y*	A	B	C	D	
TOS	-0.051	0.401E-4	0.008E-1	2.0	0.764
k_{i2}	32834.168	-138.407	-7749.457	0.1	0.594

* TOS : Total Slip (in.)

k_{i2} : Slip Modulus (lb /in.)

Subscript i denotes the order of load level (i = 1, 2, 3, 4 for 70-lb, 100-lb, 130-lb and 160-lb level, respectively)

V. CONCLUSIONS AND RECOMMENDATIONS

This study supports the following conclusions:

1. Dissipated energy and work capacity increase with increasing load.
2. The damping ratio generally decreases with increasing load except at the 1.0-Hz sinusoidal loading rate.
3. The work capacity decreases with increasing loading rate up to about 7.0-Hz. Between 7.0 and 15.0 Hz, it increases somewhat at the 70-lb load level, but it keeps on decreasing at other load levels.
4. The damping ratio moderately increases with loading rate between ASTM static and 4-Hz rate. Then it slowly decreases between 4-Hz and 15-Hz.
5. The slip decreases with increasing loading rate between ASTM and 2.5-Hz rate. Between 2.5 and 15 Hz, it increases at all load level except 160-lb.
6. Slip moduli increase with loading rate between ASTM and 2.5-Hz rate, then they decrease at all the higher rates tested. An exception is a 160-lb load level which is associated with an increase of moduli with increasing loading rate.

The recommendations of this study are:

1. Sudden impact loading after changing the load direction may affect the hysteresis loop at fast loading rates of 10 and 15 Hz. Additional testing

is recommended to define these effects.

2. In future similar testing arrangement should be improved to prevent the specimen loss. Sample size should be kept above 20.

BIBLIOGRAPHY

1. Adams, R.D. & Fox M.A. Prediction of Damping Capacity of Cast Iron from the Variation of Its Dynamic Modulus With Strain Amplitude. Journal of Iron and Steel Institute. 527-530. July 1972.

2. American Society For Testing and Materials. Annual Standards Part 22. Philadelphia, Pennsylvania. 1977.

3. Antonides, C.E., M.D. Vanderbilt, J.R. Goodman. Interlayer Gap Effects on Nail Slip Modulus. Wood Science,13(1), 41-46. 1980.

4. Atherton, George H., Kenneth E. Rowe, Ken M. Bastendorff. Damping and Slip of Nailed Joints. Wood Science, 12(4), 218-226. 1980.

5. Beyer, Williams H. CRC Standard Tables. 26th Edition, CRC Press Inc. Florida. 1984.

6. Bodig, Josef & Benjamin A. Jayne. Mechanics of Wood and Wood Composites. Van Nostrand Reinhold Co., New York. 1982.

7. Chou, Chun. Effect of Drying on Damping and Stiffness in Nailed Joints Between Wood and Plywood. M.S. Thesis, Dept. of Forest Product, Oregon State University, Corvallis, Oregon. 1984.

8. Friedrich, B., U. Teller. Structural Damping in Suspension Bridges. ASCE Paper No. 2486. 1951.

9. Foschi, R.O. Load-slip Characteristics of Nails. Wood Science, 7(1), 69-76. 1974.

10. Foschi, R.O. Load-slip Characteristics of Nails. Wood Scinece, 9(3), 118-123. 1977.

11. Groom, Leslie. Nondestructive Detection of Proportional Limit and Prediction of Destructive Parameter. M.S. Thesis, Dept. of Forest Product, Oregon State University, Corvallis, Oregon. 1985.

12. Jacobsen, L.S. Frictional Effects in Composite Structures Subjected to Earthquake Vibrations. Stanford Univ. 1959.

13. Jacobsen, L.S. Damping in Composite Structures. Proceedings. Second World Conference on Earthquake Engineering, 1029-1044. Tokyo. 1960.

14. Kaneta, K. Study of Structural Damping and Stiffness in Nailed Joints. Engineer's Thesis, Stanford Univ, Stanford, Calif. 1958.

15. Kimball, A.L. & Lovell, D.E. Internal Friction in Solid Physical Review. Second Series, Vol. 30, 948-959. 1927.

16. Loferski, T.J. Inelastic Stiffness Moduli for Nail Joints between Wood Studs and Plywood Sheathing. M.S. Thesis, Dept. of Forest Product, Oregon State University, Corvallis, Oregon. 1981.

17. Medearis, K.G. An Investigation of the Structural Damping Characteristics of Composite Wood Structures Subjected to Cyclic Loading. Ph.D. Thesis. Dept. of Civil Engineering, Stanford Univ., Stanford, Calif. 1962.

18. Medearis, K.G. An Investigation of the Static and Dynamic Characteristics of Shear Wall Response. Report submitted to Calif. Highway Dept., Sunnyvale, Calif. 1966.

19. Metherell, A.F. Instantaneous Energy Dissipation Rate in a Lap Joint Uniform Clamping Pressure. Journal of Applied Mechanics, 123-128. March, 1968.

20. Nie, Norman H.; Hull, C. Hadlai; Jenkins, J.G.; Steinbrenner, K.; Bent, D.H. SPSS-Statistical Packages for the Social Science. Second Edition, McGraw Hill, New York. 1975.

21. Pellicane, P.J. & Jozsef Bodig. Comparative Study of Several Testing Techniques to Evaluate Nail-Slip Modulus. Special Report SWL-1. Dept. of Forest and Wood Sciences, Colorado State Univ, Fort Collins Co. 1982.

22. Polensek, Anton & Harold I. Laursen. Seismic Behavior of Bending Components and Intercomponent Connections of Light Frame Wood Building. Limited Distribution Report. Forest Research Laboratory, Oregon State University, Corvallis, Oregon. 1984.

23. Polensek, Anton. Compression-bending Tests of Walls with Utility Grade Englemann Spruce Studs and Properties for Two Species of Utility Grade Studs. Forest Research Laboratory, Oregon State University, Corvallis, Oregon. June, 1973.

24. Polensek, Anton. Damping Capacity of Nailed Wood-joint Floors. Wood Science, 8(2), 141-151. 1975.

25. Polensek, Anton. Static and Dynamic Properties of Glued Wood-joist Floors. Forest Product Journal, 21(12), 31-39. 1971.

26. Ungar, E.E. The status of Engineering Knowledge Concerning the Damping of Built Up Structure. Journal of Sound and Vibration, 26(1), 141-154. 1973.

27. U.S. Department of Agriculture, Forest Product Laboratory. Wood Handbook, U.S. Government Printing Office, Washington D.C. 1955.

28. Wilkinson, T.L. Analysis of Nailed Joints with Dissimilar Members. Journal of Structural Division of ASCE, 2005-2013. 1972.

29. Wilkinson, T.L. Theoretical Lateral Resistance of Nailed Joints. Journal of Structural Division of ASCE, 1381-1389. May, 1971.

30. Yeh, C.T. A study on the Mechanisms of Damping in Wood Structure. Ph.D. Thesis. Department of Civil Engineering, University of Washington, 1970.

31. Yeh, C.T. Damping Source in Wood Structures. Journal of Sound and Vibration, 19(4), 411-419. 1971.

APPENDICES

Appendix A

Computer Program for Data Reduction

```
      PROGRAM ANALY
C
C     THIS PROGRAM OUTPUTS DATA FROM TESTS IN TABULAR FORM.
C
      INTEGER*2 IGID(8,5),BUF1(1200),BLKNO,IDATE(5),ITIME(5)
      DIMENSION IDATA(40),IGAIN(8),GAIN(4),DISP(8),SENS(8)
     +         ,T(2400),D(2400),DCY(900),TCY(900)
      DATA GAIN/0.000488,0.000976,0.00244,0.00488/
C
C     CONNECT DX2 FOR READ
C
      TYPE 5
5     FORMAT( '$ ENTER SOURCE FILE NAME..')
      CALL ASSIGN(2,DK2,-1)
      DEFINE FILE 2(43,1200,U,NREC)
C
C     READ HEADER INFO AND DISPLAY IT
C
      READ(2'1) (BUF1(I),I=1,1200)
      NBLOC=BUF1(1)
      NCHAN=BUF1(2)
      DO 10 I=1,5
10    IDATE(I)=BUF1(I+2)
      DO 11 I=1,4
11    ITIME(I)=BUF1(I+7)
      DO 12 I=1,8
12    IGAIN(I)=BUF1(I+11)
      DO 13 J=1,8
      DO 13 I=1,5
      IGID(J,I)=BUF1(I+19+(J-1)*5)
13    CONTINUE
      IFREQ=BUF1(60)
      DO 14 I=1,40
14    IDATA(I)=BUF1(I+60)
C
C     INPUT SENSITIVITIES
C
      DO 15 J=1,NCHAN
      WRITE(7,16) (J-1),(IGID(J,K),K=1,5)
16    FORMAT( ' INPUT SENSITIVITY FOR CHANNELM ',I2,':',5A2,' ')
```

```
      READ(7,17) SENS(J)
17    FORMAT(F11.6)
15    CONTINUE
C
C     INPUT BLOCK NUMBERS TO BE READ
C
      TYPE 18
18    FORMAT( '$INPUT FIRST BLOCK NO. TO BE PRINTED..')
      READ(7,19) INITIA
19    FORMAT(I3)
      TYPE 20
20    FORMAT( '$ INPUT LAST BLOCK NO. TO BE PRINTED..')
      READ(7,21) LASTBL
21    FORMAT(I3)
      WRITE(7,22)
22    FORMAT( '$INPUT SAMPLING INTERVAL..')
      READ(7,23) ISAMPI
23    FORMAT(I3)
C
C     OUTPUT HEADER INFO
C
      WRITE(7,24) (BUF1(I), I=61,100)
24    FORMAT(1X,40A2)
      WRITE(7,25) (IDATE(I), I=1,5)
25    FORMAT(' DATE ',5A2)
      WRITE(7,30) IFREQ
30    FORMAT( ' FREQUENCY=',I3,' HZ')
      DO 130 I=1,NCHAN
      II=I-1
      TYPE 135,II,(IGID(I,J),J=1,5),IGAIN(I),SENS(I)
135   FORMAT(' CHAN# ',I2,': ',5A2,' @ GAIN= ',I2,' SENSITIVITY=',
     + F7.3)
130   CONTINUE
      WRITE(7,132) INITIA
132   FORMAT( ' FIRST BLOCK = ',I3)
      WRITE(7,134) LASTBL
134   FORMAT( ' LAST BLOCK = ',I3)
      WRITE(7,136) ISAMPI
136   FORMAT( ' SAMPLING INTERVAL = ',I3)
C
C     READ TEST DATA AND OUTPUT
C
      WRITE(7,147)
147   FORMAT(' TIME                    CHANNEL#')
      WRITE(7,148) IFREQ
148   FORMAT('/SEC*',I4,'HZ',3X,'0',12X,'1',11X,'2',13X,'3',13X,'4',
     + 13X,'5',12X,'6',13X,'7')
      LASTBL=LASTBL+1
      IBLKNO=INITIA
5000  CONTINUE
      IBLKNO=IBLKNO+1
```

```
      IF(IBLKNO.GT.LASTBLK)GO TO 5001
      III=1
      WRITE(7,5010)IBLKNO
5010  FORMAT(I4)
      FIND (2'IBLKNO)
      READ(2'IBLKNO,END=299) (BUF1(I),I=1,1200)
      J=MOD((1200*(IBLKNO-2)),(NCHAN*ISAMPI))+1
      KINITI=MOD((1200/NCHAN)*(IBLKNO-2),ISAMPI)+1
      DO 200 K=KINITI,(1200/NCHAN),ISAMPI
      L=0
      DO 149 I=J, (J+NCHAN-1)
      L=L+1
      DISP(L)=BUF1(I)*GAIN(IGAIN(L)+1)/SENS(L)
149   CONTINUE
      J=J+(NCHAN*ISAMPI)
      T(III)=DISP(1)
      D(III)=DISP(2)
        III=III+1
200   CONTINUE
C
C     READ DATA AND DETERMINE POINT
C
      DO 1002 I=1,600
      IF(T(I)*T(I+1).LE.0 .AND.(T(I+1)T(I+2)).GT.0)GO TO 201
1002  CONTINUE
201   LA=I+1
      TA=T(I+1)
      DA=D(I+1)
      DO 4000 II=1,12
      J=0
      DO 1004 I=(LA+1),600
      J=J+1
      DCY(J)=D(I)
      TCY(J)=T(I)
1004  CONTINUE
      DO 8001 I=2,(600-LA)
      IF(DCY(I)*DCY(I-1).LE.0)GO TO 380
8001  CONTINUE
      GO TO 4001
380   NP=I-1
      TF=TCY(I)
      DF=DCY(I)
      DO 1005 I=2,(600-LA)
      IF((TCY(I+1)+TCY(I+2)+TCY(I+3)+TCY(I+4)).LT.(TCY(I)
     + +TCY(I-1)+TCY(I-2)+TCY(I-3)).AND.TCY(I).GT.60.)GO TO 202
1005  CONTINUE
      GO TO 4001
202   NO=I-NP
      TB=TCY(I-1)
      DB=DCY(I-1)
      ND=NO+NP
```

```
      DO 1007 I=(ND+2),(600-LA)
      IF(TCY(I-1)*TCY(I).LE.0 .AND. (TCY(I+1)+TCY(I)).LT.0)GO TO 203
1007  CONTINUE
      GO TO 4001
203   ND2=I-ND
      TE=TCY(I)
      DE=DCY(I)
      ND2=ND2+ND
      DO 1009 I=(ND2+2),(600-LA)
      IF((TCY(I+1)+TCY(I+2)+TCY(I+3)+TCY(I+4)).GT.(TCY(I)
     + +TCY(I-1)+TCY(I-2)+TCY(I-3)))GO TO 204
1009  CONTINUE
      GO TO 4001
204   NDC=I-ND2
      TD=TCY(I)
      DD=DCY(I)
      NDC=NDC+ND2
      WRITE(7,4802)NDC
4802  FORMAT(I5)
      DO 1011 I=(NDC+2),(600-LA)
      IF(TCY(I)*TCY(I-1).LE.0 .AND.(TCY(I)+TCY(I+1)).GT.0)GO TO 205
1011  CONTINUE
      GO TO 4001
205   NDC2=I-NDC
      TC=TCY(I)
      DC=DCY(I)
C
C     READ DATA AND CALCULATE AREA,DAMPING RATIO
C
      WRITE(7,150)ND,ND2,NDC,NDC2
150   FORMAT(4I5)
      PI=3.141592
      UTN=.25*TB*(DB-DD)
      TLTN=.25*(ABS(TD))*(DB-DD)
      SA=(TB-TD)/(DB-DD)
      SB=(TB-TE)/(DB-DE)
      SC=(TB-TF)/(DB-DF)
      WRITE(7,8002)SA,SB,SC
8002  FORMAT(2X,'SA=',F10.2,2X,'SB=',F10.2,2X,'SC=',F10.2)
      DI=(DB-DA)/ND
      NND=ND-1
      AU=0.
      DO 1013 I=1,NND
      A=DI*(TCY(I)+TCY(I+1))*.5
      AU=AU+A
1013  CONTINUE
      NND2=ND2-1
      DI=(DB-DE)/(ND2-ND)
      AL=0.
      DO 1014 I=ND,NND2
      A=DI*(TCY(I)+TCY(I+1))*.5
```

```
      AL=AL+A
1014  CONTINUE
      PNTA=AU-AL
      RTC=PNTA/UTN/PI*.5
      WRITE(7,400) RTC
400   FORMAT('UPPER D-RATIO=',F8.4)
      DI=(DE-DD)/(NDC-ND2)
      AP=0.
      NNDC=NDC-1
      DO 1015 I=ND2,NNDC
      A=DI*(ABS(TCY(I))+ABS(TCY(I+1)))*.5
      AP=AP+A
1015  CONTINUE
      DI=(DC-DD)/NDC2
      AO=0.
      NNDC2=NDC2-1+NDC
      DO 1016 I=NDC,NNDC2
      A=DI*(ABS(TCY(I))+ABS(TCY(I+1)))*.5
      AO=AO+A
1016  CONTINUE
      PNTLA=AP-AO
      RLTC=PNTLA/TLTN/PI*.5
      WRITE(7,500)RLTC
500   FORMAT(2X,'LOWER D-RATIO='F10.7)
C
C     OUTPUT DAMPING RATIO AND POINT
C
      WRITE(7,8004)TF,DF
8004  FORMAT(F10.3,2X,F10.3)
      WRITE(7,600) TA,DA,TB,DB,TE,DE,TD,DD,TC,DC
600   FORMAT(10E13.3)
      TATD=PNTA+PNTLA
      TTA=UTN+TLTN
      RTO=TATD/TTA/PI*.5
      WRITE(7,700)PNTA,PNTLA,UTN,TLTN,TATD,TTA,RTO
700   FORMAT(/'UPPER AREA=',E13.3,2X,'LOWER AREA=',E13.3/
     +  'UPPER TRI. ARES=',E13.3,2X,'LOWER TRI.AREA=',E13.3,2X,
     +  /'TOTAL AREA=',E13.3,2X,'TOTAL TRI.AREA=',E13.3,2X,
     +  /'RATIO OF TOTAL AREAS=',E13.3)
      III=1
      TA=TC
      DA=DC
      LA=NDC2+NDC+LA
4000  CONTINUE
4001  CONTINUE
      GO TO 5000
299   WRITE(7,300)
300   FORMAT(' EOF DURING FILE READ')
5001  STOP 'DONE'
      END
```

Appendix B

Scattergram of Damping Ratio

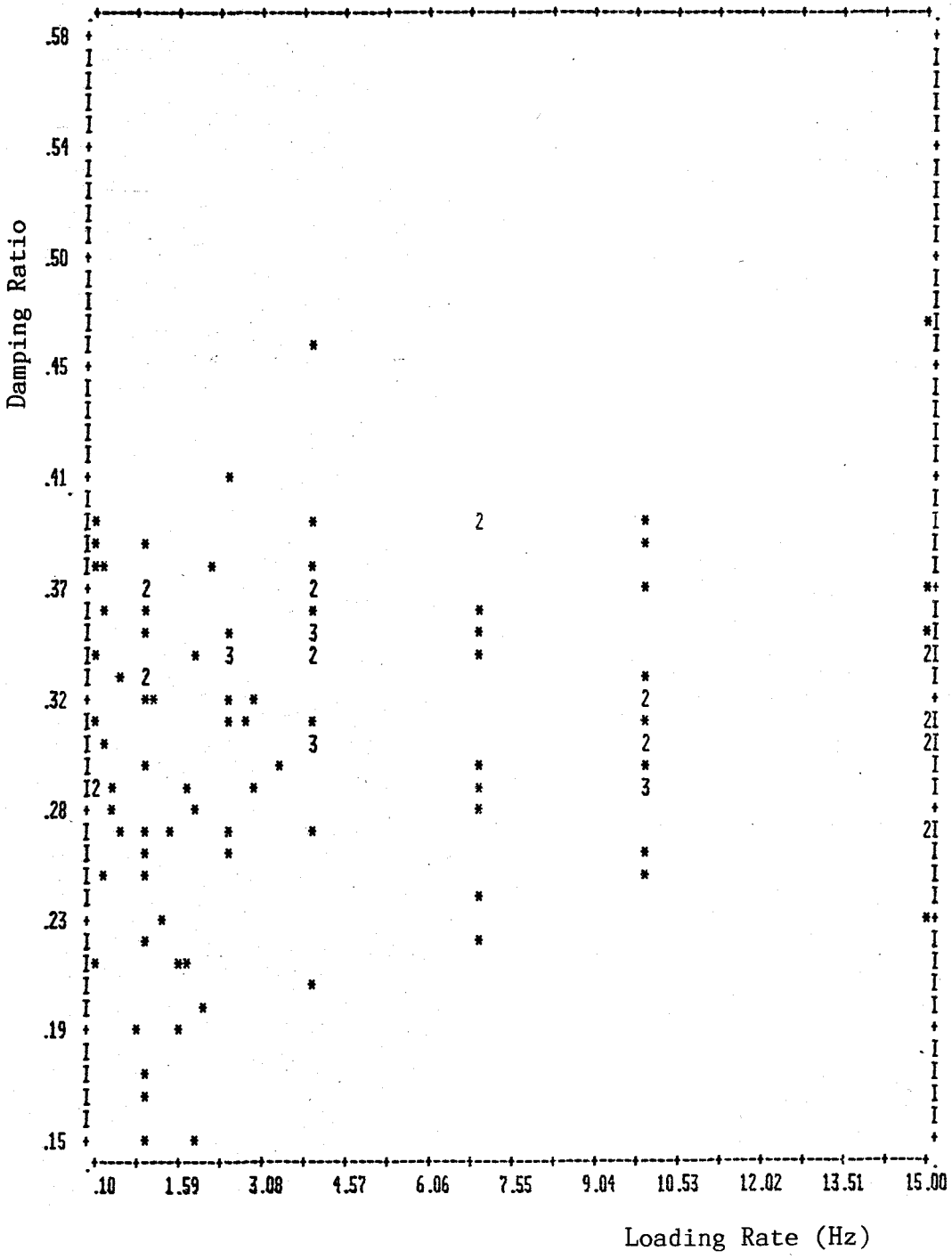

Figure B.1. Scattergram between Damping Ratio and Loading Rate for 70-lb Load Level

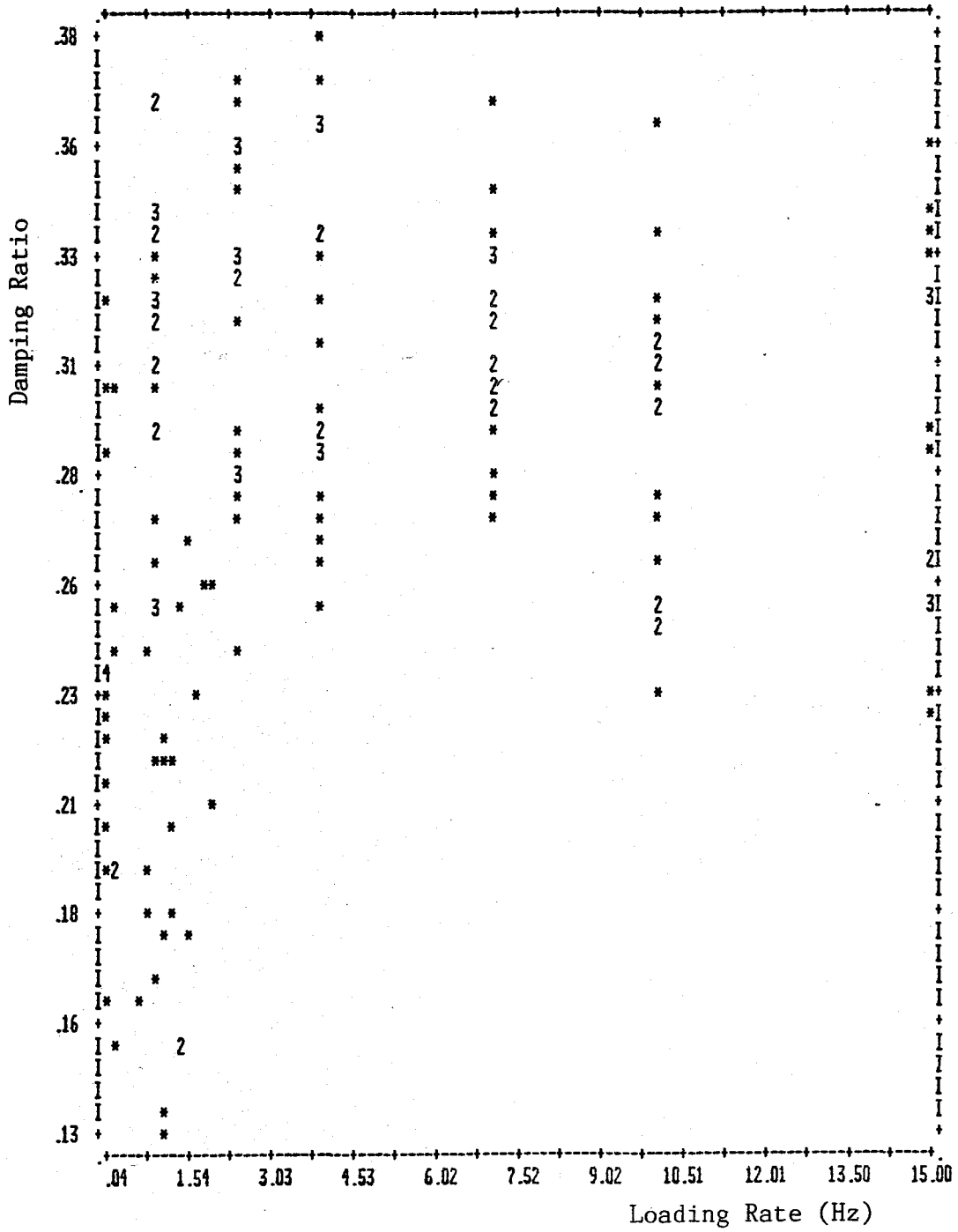

Figure B.2. Scattergram between Damping Ratio and Loading Rate for 100-lb Load Level

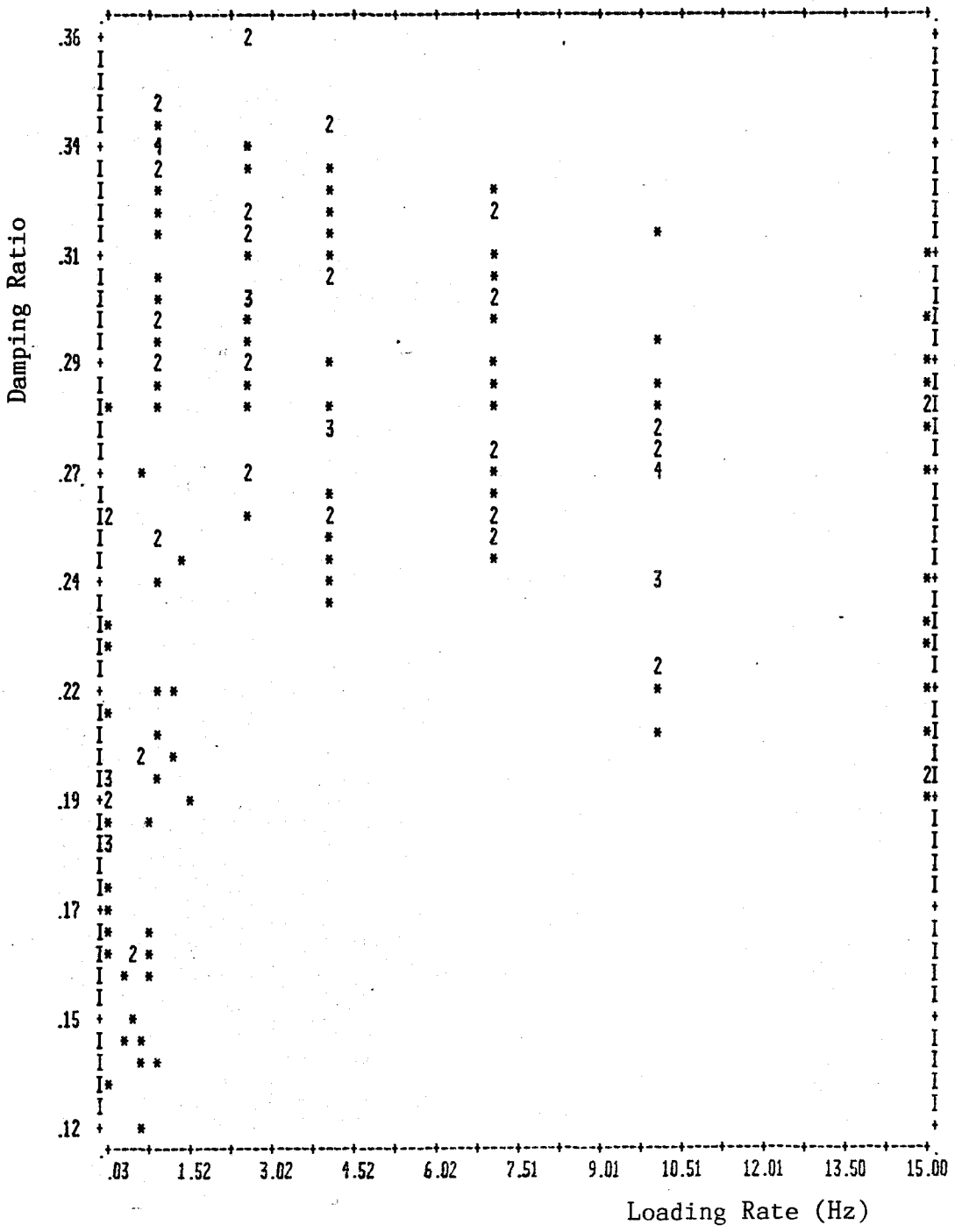

Figure B.3. Scattergram between Damping Ratio and Loading Rate for 130-lb Load Level

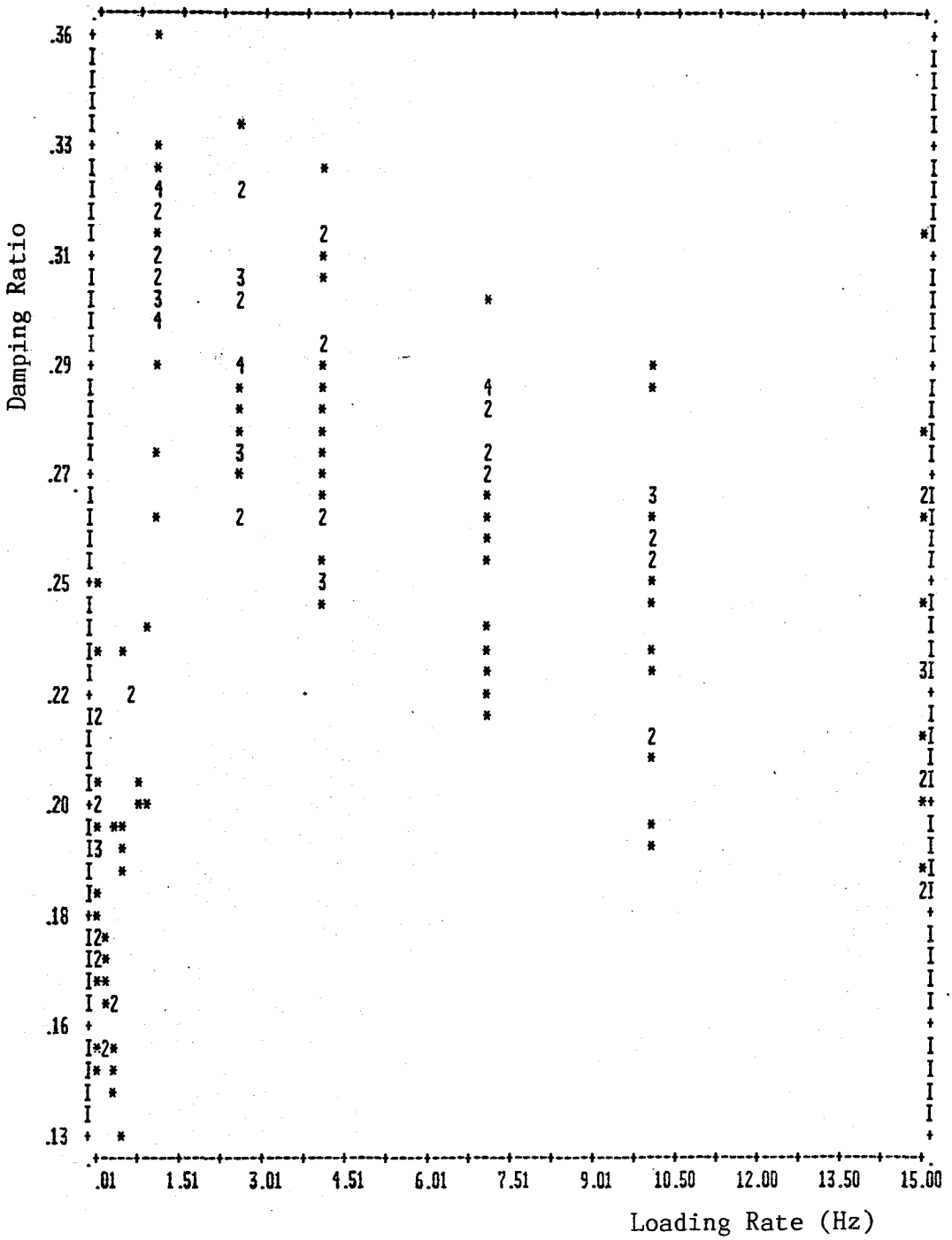

Figure B.4. Scattergram between Damping Ratio and Loading Rate for 160-lb Load Level

Appendix C

Results from T-Test

Table C.1. T-Test Comparing the Damping Ratios at Two Loading Rates for 70-lb Load Level

Loading Rate*	T-statistic**	Loading Rate						
		0.15 in/min	1.5 in/min	1.0 Hz	2.5 Hz	4.0 Hz	7.0 Hz	10.0 Hz
1.5 in/min	C	2.68						
	L	2.04						
1.0 Hz	C	1.24	0.99					
	L	2.04	2.04					
2.5 Hz	C	0.91	3.00	1.63				
	L	2.06	2.05	2.07				
4.0 Hz	C	1.22	3.81	2.22	0.17			
	L	2.04	2.03	2.04	2.07			
7.0 Hz	C	0.87	2.62	1.60	0.17	0.09		
	L	2.06	2.05	2.06	2.11	2.05		
10.0 Hz	C	0.12	2.73	1.20	1.18	1.42	0.97	
	L	2.04	2.03	2.04	2.08	2.04	2.06	
15.0 Hz	C	0.39	2.66	1.37	0.44	0.66	0.50	0.52
	L	2.06	2.05	2.06	2.10	2.05	2.08	2.06

* Sample sizes identified in table 4.1

** C = Computed T-statistic

L = Limit T-statistic at 0.05-level

Significant at 0.05-level if C > L

Table C.2. T-Test for Comparing the Damping Ratios at Two Loading Rates for 100-lb Load Level

Loading Rate*	T-statistic**	Loading Rate						
		0.15 in/min	1.5 in/min	1.0 Hz	2.5 Hz	4.0 Hz	7.0 Hz	10.0 Hz
1.5 in/min	C	1.95						
	L	2.02						
1.0 Hz	C	5.92	8.10					
	L	2.02	2.01					
2.5 Hz	C	6.66	8.74	1.00				
	L	2.02	2.02	2.02				
4.0 Hz	C	5.96	8.01	0.39	0.57			
	L	2.02	2.02	2.02	2.02			
7.0 Hz	C	7.04	9.16	0.56	0.58	0.10		
	L	2.02	2.02	2.02	2.02	2.02		
10.0 Hz	C	4.56	6.61	1.44	2.42	1.76	2.32	
	L	2.03	2.02	2.02	2.02	2.02	2.03	
15.0 Hz	C	3.98	5.80	1.24	2.08	1.51	1.93	0.01
	L	2.03	2.03	2.02	2.03	2.03	2.03	2.03

* Sample sizes identified in table 4.1

** C = Computed T-statistic

L = Limit T-statistic at 0.05-level

Significant at 0.05-level if C > L

Table C.3. T-Test for Comparing the Damping Ratios at Two Loading Rates for 130-lb Load Level

Loading Rate*	T-statistic**	Loading Rate						
		0.15 in/min	1.5 in/min	1.0 Hz	2.5 Hz	4.0 Hz	7.0 Hz	10.0 Hz
1.5 in/min	C	1.60						
	L	2.02						
1.0 Hz	C	10.08	11.61					
	L	2.02	2.01					
2.5 Hz	C	10.52	11.87	0.15				
	L	2.02	2.02	2.02				
4.0 Hz	C	8.07	9.53	1.86	1.82			
	L	2.02	2.02	2.02	2.02			
7.0 Hz	C	8.34	9.73	2.42	2.48	0.41		
	L	2.02	2.02	2.02	2.02	2.02		
10.0 Hz	C	5.70	7.16	4.85	5.13	2.87	2.75	
	L	2.03	2.02	2.02	2.02	2.02	2.03	
15.0 Hz	C	4.01	5.36	4.80	4.95	3.10	3.00	0.77
	L	2.03	2.03	2.02	2.03	2.03	2.03	2.03

* Sample sizes identified in table 4.1

** C = Computed T-statistic

L = Limit T-statistic at 0.05-level

Significant at 0.05-level if C > L

Table C.4. T-Test for Comparing the Damping Ratios at Two Loading Rates for 160-lb Load Level

Loading Rate*	T-statistic**	Loading Rate						
		0.15 in/min	1.5 in/min	1.0 Hz	2.5 Hz	4.0 Hz	7.0 Hz	10.0 Hz
1.5 in/min	C L	0.98 2.02						
1.0 Hz	C L	17.06 2.02	16.88 2.01					
2.5 Hz	C L	13.64 2.02	13.63 2.02	2.80 2.02				
4.0 Hz	C L	10.56 2.02	10.97 2.02	4.43 2.02	1.83 2.02			
7.0 Hz	C L	9.08 2.02	9.45 2.02	7.04 2.02	4.15 2.02	1.97 2.02		
10.0 Hz	C L	6.08 2.03	6.66 2.02	9.22 2.02	6.38 2.02	4.14 2.02	2.41 2.03	
15.0 Hz	C L	3.84 2.03	4.50 2.03	8.61 2.02	6.25 2.03	4.45 2.03	3.04 2.03	1.03 2.03

* Sample sizes identified in table 4.1

** C = Computed T-statistic

L = Limit T-statistic at 0.05-level

Significant at 0.05-level if C > L